

UNCLASSIFIED

AD NUMBER

AD851944

LIMITATION CHANGES

TO:

Approved for public release; distribution is unlimited.

FROM:

Distribution authorized to U.S. Gov't. agencies and their contractors; Critical Technology; FEB 1969. Other requests shall be referred to Air Force Rome Air Development Center, EMATE, Griffiss AFB, NY 13440. This document contains export-controlled technical data.

AUTHORITY

radc, usaf, ltr, 17 sep 1971

THIS PAGE IS UNCLASSIFIED

RADC-TR-69-93
February 1969



AD851944

CHARACTERIZATION OF THE MICROWAVE TENSOR PERMEABILITY OF PARTIALLY MAGNETIZED MATERIALS

Jerome J. Green
Ernst Schlömann
Frank Sondy
Joseph Saunders

Contractor: Raytheon Company, Research Division
Contract Number: F30602-69-C-0026
Effective Date of Contract: 2 August 1968
Contract Expiration Date: 2 August 1969
Amount of Contract: \$59,464.00
Program Code Number: 8E30

Principal Investigator: J. J. Green
Phone: AC 717 899-8400 X2475

Project Engineer: P. A. Romanelli
Phone: AC 315 330-4251

Sponsored By
Advanced Research Projects Agency
ARPA Order No. 550
Amendment No. 6

This document is subject to special
export controls and each transmittal
to foreign governments, foreign na-
tionals or representatives thereto may
be made only with prior approval of
RADC (EMATE), GAFB, N.Y. 13440.

Rome Air Development Center
Air Force Systems Command
Griffiss Air Force Base, New York

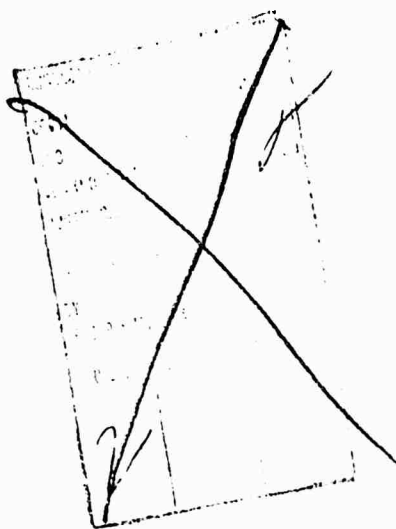
Reproduced by
NATIONAL TECHNICAL
INFORMATION SERVICE
U S Department of Commerce
Springfield VA 22151

This document has been approved
for public release and sale; its
distribution is unlimited

A

4

When US Government drawings, specifications, or other data are used for any purpose other than a definitely related government procurement operation, the government thereby incurs no responsibility nor any obligation whatsoever; and the fact that the government may have formulated, furnished, or in any way supplied the said drawings, specifications, or other data is not to be regarded, by implication or otherwise, as in any manner licensing the holder or any other person or corporation, or conveying any rights or permission to manufacture, use, or sell any patented invention that may in any way be related thereto.



Do not return this copy. Retain or destroy.

CHARACTERIZATION OF THE MICROWAVE TENSOR PERMEABILITY
OF PARTIALLY MAGNETIZED MATERIALS

Jerome J. Green

Ernst Schlömann

Frank Sandy

Joseph Saunders

Raytheon Research Division

This document is subject to special
export controls and each transmittal
to foreign governments, foreign na-
tionals or representatives thereto may
be made only with prior approval of
RADC (EMATE), GAFB, N.Y. 13440.

This research was supported by the
Advanced Research Projects Agency
of the Department of Defense and was
monitored by Patsy A. Romanelli,
RADC (EMATE), GAFB, N.Y. 13440
under Contract F30602-69-C-0026

FOREWORD

This study is being performed at Raytheon Company's Research Division, 28 Seyon Street, Waltham, Massachusetts 02154, for the Advanced Research Projects Agency, Washington, D.C. Rome Air Development Center, Griffiss Air Force Base, New York is monitoring the study for ARPA under Contract F30602-69-C-0026. Mr. P. A. Romanelli, EMATE, is the RADC Project Engineer.

The distribution of this report is limited under the US Export Control Act of 1949.

This technical report has been reviewed and is approved.

Patsy A. Romanelli

RADC Project Engineer
PATSY A. ROMANELLI

ABSTRACT

The loss for a partially magnetized material can be characterized by μ'' of the completely demagnetized state if $\omega_M/\omega \leq 0.7$. Results are presented for a number of yttrium iron garnets with aluminum and gadolinium substitutions and magnesium manganese spinels with aluminum substitutions. μ'' has been measured at frequencies of 5.5, 7.3, 9.0, 11.4, 13.8, 16.9 GHz. The results can be approximated by a relation $\mu'' = A(\omega_M/\omega)^N$. The YAlG materials are low in loss, MgMnAlF slightly higher, and the YGDAlG considerably higher in loss. Two theoretical modes have been developed which are an improvement over Rado's theory and give qualitative descriptions of the partially magnetized permeability tensor.

High-power parallel-pump measurements have been made on the same materials at frequencies of 5.5 and 9.2 GHz and at fields of 0, $4\pi M_s/3$, and H_{\min} . These materials have the same ranking with respect to threshold as they have for low-power loss.

TABLE OF CONTENTS

	<u>Page</u>
I: INTRODUCTION.....	1
II. PERMEABILITY TENSOR OF PARTIALLY MAGNETIZED MAGNETIC MATERIALS.....	2
III. THE HIGH POWER PROPERTIES OF PARTIALLY MAGNETIZED MATERIALS.....	9
REFERENCES.....	13
Appendix 1 - Permeability of Partially Magnetized Ferrites	14
Appendix 2 - Microwave Behavior of Partially Magnetized Ferrites	33



LIST OF ILLUSTRATIONS

<u>Number</u>	<u>Title</u>	<u>Page</u>
1	μ'' vs ω_M/ω at $4\pi M = 0$ for Various Garnets and Mg Ferrites	3
2	μ' vs ω_M/ω at $4\pi M = 0$ for Various Garnets and Mg Ferrites	7

LIST OF TABLES

<u>Number</u>	<u>Title</u>	<u>Page</u>
I	Loss Parameters of Garnets and Magnesium Ferrites	5
II	Parallel Pump - 5.5 GHz	10
III	Parallel Pump - 9.2 GHz	11



SECTION I

INTRODUCTION

Modern radar and communication systems are putting requirements on microwave ferrite devices which are a test of the ingenuity of the device designer and the materials physicist. Phased-array systems require temperature stability, cheapness, reproducibility, and light weight. Low insertion loss and high peak-power performance are highly desirable. The driving circuits must be simple, dependable, and inexpensive. There is also a trend to miniaturization and integration. In any given application, it is impossible to maximize every single one of these performance characteristics simultaneously and therefore some sort of a trade-off procedure is required.

In order to be able to make a performance trade-off, it is necessary to be able to predict the effect of design procedures upon performance characteristics. The goals of the present program are to study how the permeability of partially magnetized materials depends on material parameters and to catalogue the loss properties of a number of the important phase shifting materials. It should then be possible to use computer-aided design procedures in the trade-off procedure.

The results of the last half year are reported in two sections. The first section deals with the low power loss parameter μ'' of the demagnetized state as measured on a number of materials across a range of frequencies. Previous work has determined the dependence of real parts of the permeability tensor upon material parameters. This permits phase-shifting calculations. The present work permits the calculation of insertion loss. The second section deals with the high-power performance of these same materials.

SECTION II

PERMEABILITY TENSOR OF PARTIALLY MAGNETIZED MAGNETIC MATERIALS

One of the purposes of this contract has been to describe the loss part of permeability tensor for a wide variety of materials in partially magnetized states. Earlier measurements of μ'' and κ'' about the hysteresis loop¹ have shown that when $\omega_M/\omega < 0.7$, $\kappa'' \ll \mu''$. This is confirmed theoretically by calculations of Schlömann described in an appendix to this report. In addition, it was found that μ'' is relatively insensitive to position on the hysteresis loop in this region. Only a shallow minimum at $4\pi M = 0$ is observed. Measurements of μ_z'' have shown¹ that it has a maximum at $4\pi M = 0$ where it equals μ'' . It is thus reasonable to characterize the partially magnetized states by a single loss constant (when $\omega_M/\omega < 0.7$), namely μ'' at $4\pi M = 0$ which is nearly an upper limit on all of the loss terms.

Measurements of μ'' in the demagnetized state have been made on seven garnets with various amounts of aluminum and gadolinium substitution and on five magnesium ferrites with various amounts of aluminum substitution. The samples had magnetizations ranging from 725 to 2475 gauss. Most of the samples were measured at six frequencies from 5.5 to 16.7 GHz. This covered ω_M/ω ratios from 0.11 to 0.89. The measurements were made on thick slabs in a rectangular cavity as described in Ref. 1. Thick slabs rather than the more conventional rod- or sphere-shaped samples were used to improve sensitivity in the region $\mu'' < 10^{-4}$. The results are displayed in Fig. 1 on a log-log plot of μ'' vs ω_M/ω . The experimental accuracy is believed to be comparable to the scatter from the interpolated curves, namely $\pm (10 \text{ percent} + 0.00001)$. The data follows a simple power law relationship:

$$\mu''_{\text{demag}} = A \left(\frac{\omega_M}{\omega} \right)^N \quad (1)$$

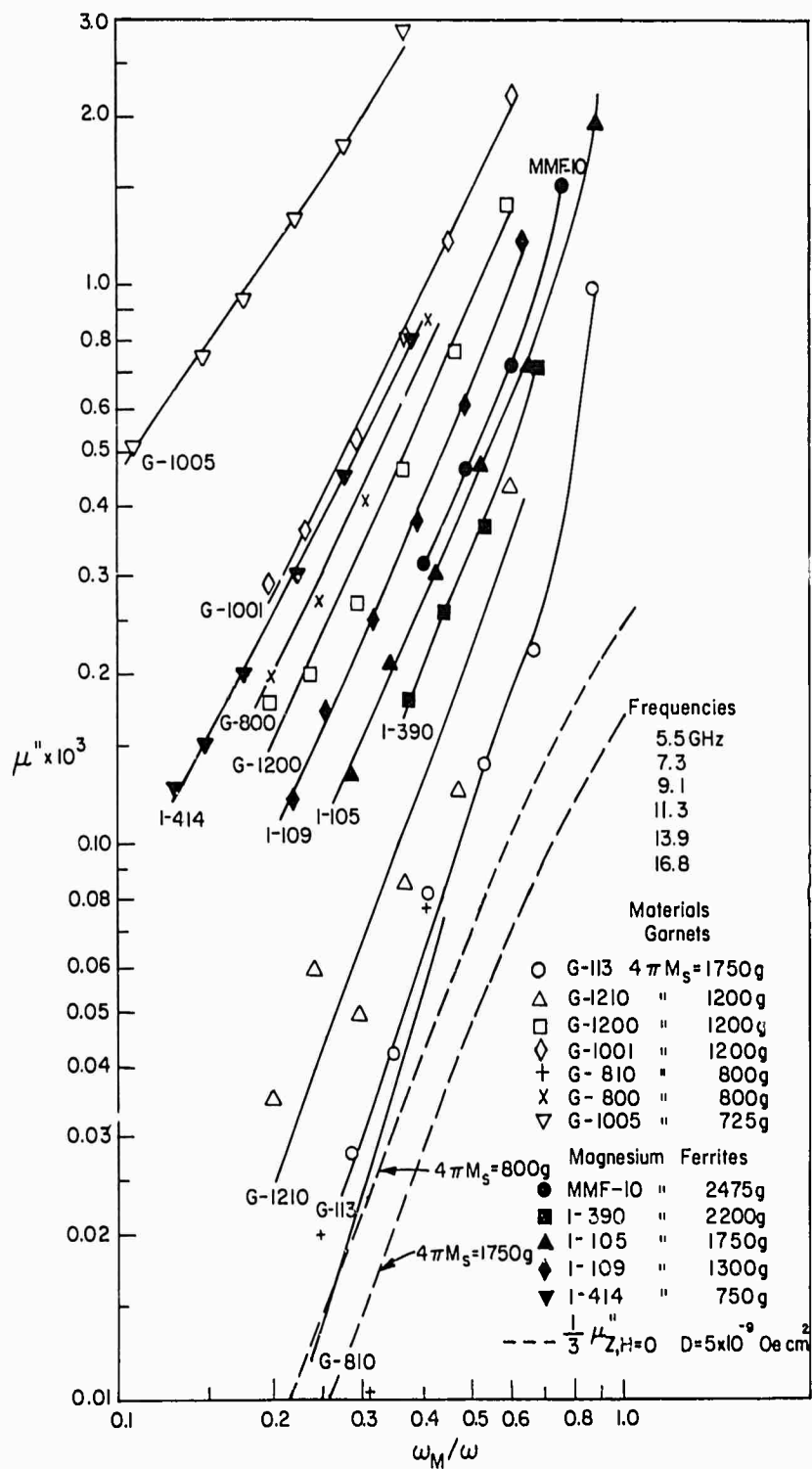


Fig. 1 μ'' vs ω_M/ω at $4\pi M = 0$ for Various Garnets and Mg Ferrites

for all $\omega_M/\omega < 0.7$. At greater ratios of ω_M/ω , μ'' increases more rapidly, becoming extremely large as ω_M/ω approaches 1.0. The measured values of A and N are listed in Table I. It should be noted that increases in gadolinium content in YIG and increases in aluminum content in MgMn ferrite increase A and decrease N, whereas an increase in aluminum content in YIG has little effect on loss other than through the change in magnetization.

For a saturated sample at zero field

$$\mu''_{H=0} = \frac{\gamma \Delta H_{\text{eff}}}{2} \frac{\omega_M}{\omega^2} \quad (2)$$

where $\Delta H_{\text{eff}} = 2/\gamma T$ is an effective linewidth proportional to the intrinsic relaxation rate of the material, not the ferromagnetic resonance linewidth. A subthreshold parallel pump loss at zero field has been derived by Joseph and Schlömann.² Their results show that $\mu''_{Z, H=0}$ depends on ω_M/ω , temperature, and the exchange constant, but not on ΔH_{eff} . In the demagnetized state, 1/3 of the domains are being parallel pumped and 2/3 of the domains are being perpendicularly pumped. We may thus assume that μ'' in the demagnetized state with ω_M/ω well below 1.0 is given by:

$$\mu''_{\text{demag}} = \frac{2}{3} \mu''_{H=0} + \frac{1}{3} \mu''_{Z, H=0} \quad (3)$$

The term $1/3 \mu''_{Z, H=0}$ is plotted in Fig. 1 for $4\pi M_s = 800$ and 1750 gauss using the exchange constant of YIG ($D = 5 \cdot 10^{-9}$ Oe-cm²).

From our results it appears that for the very low-loss materials G-113, G-810, and G1210, i.e., those having the lowest value of A, a significant part of μ''_{demag} arises from the subthreshold parallel pump loss. For the higher loss materials the μ''_{demag} arises almost entirely from the usual perpendicular pump loss.

TABLE I
LOSS PARAMETERS OF GARNETS AND MAGNESIUM FERRITES

<u>Material</u>	<u>Composition</u>	$4\pi M_s$ (gauss)	<u>A</u>	<u>N</u>	ΔH_{eff} at $\omega_M/\omega = 1.0$ (Oe)
G-113	YIG	1750	$7.5 \cdot 10^{-4}$	2.5	3.0
G-1210	YIG + Al	1200	10.0	2.4	3.0
G-1200	YIG + Al + Gd	1200	34.0	1.9	12.0
G-1001	YIG + Gd	1200	50.0	1.8	18.0
G-810	YIG + Al	800	8.0	2.8	1.5
G-800	YIG + Al + Gd	800	43.0	1.9	15.0
G-1005	YIG + Gd	725	95.0	1.3	21.0
MMF-10	MgMn ferrite	2475	20.0	2.0	15.0
1-390	MgMn ferrite with second phase	2200	16.0	2.2	11.0
1-105	MgMn ferrite + Al	1750	18.0	2.0	9.0
1-109	MgMn ferrite + Al	1300	28.0	1.9	11.0
1-414	MgMn ferrite + Al	750	45.0	1.7	10.0

Combining Eqs. (1-3) we may set

$$\frac{2}{3} \frac{\gamma \Delta H_{\text{eff}}}{2} \frac{\omega_M}{\omega} + \frac{1}{3} \mu_{z, H=0}'' = A \left(\frac{\omega_M}{\omega} \right)^N \quad (4)$$

or

$$\Delta H_{\text{eff}} = 4\pi M_s \left(\frac{\omega_M}{\omega} \right)^{-2} \left\{ 3A \left(\frac{\omega_M}{\omega} \right)^N - \mu_{z, H=0}'' \right\} \quad (5)$$

When the parallel pump term is small, (N-2) gives the frequency dependence of ΔH_{eff} . The values of ΔH_{eff} at $\omega_M/\omega = 1.0$ are easily obtained from Eq. (5) and are tabulated in Table I.

Measurements of μ' on the same materials were made at each frequency at the same time as the μ'' measurements. The measured values of μ' are plotted vs ω_M/ω in Fig. 2, and it can be seen that the points for all the materials fall close to a single curve. Also included in this figure are some of the measurements of μ' on demagnetized magnesium ferrite at a single frequency, 5.5 GHz, reported in Ref. 1. In these measurements, temperature (and hence ω_M) was varied.

A theory of the partially magnetized state proposed by Sandy is appended to this report. It extends Rado's³ earlier theory of the partially magnetized state to include correlation between internal demagnetizing fields and domain orientations. This results in substantially improved relations for μ' and μ_z' vs $\gamma 4\pi M/\omega$ and $\gamma 4\pi M_s/\omega$. In particular for the demagnetized state it yields

$$\mu' = \mu_z' = 1 - \frac{\frac{2}{3} N (\omega_M + \gamma H_a/N)^2 / \omega}{1 - \frac{1}{3} N^2 (\omega_M + \gamma H_a/N)^2 / \omega^2} \quad (6)$$

where N is an average demagnetizing factor and H_a is an average anisotropy field. The best fit to the data in Fig. 2 for $\omega_M/\omega < 0.9$ is obtained

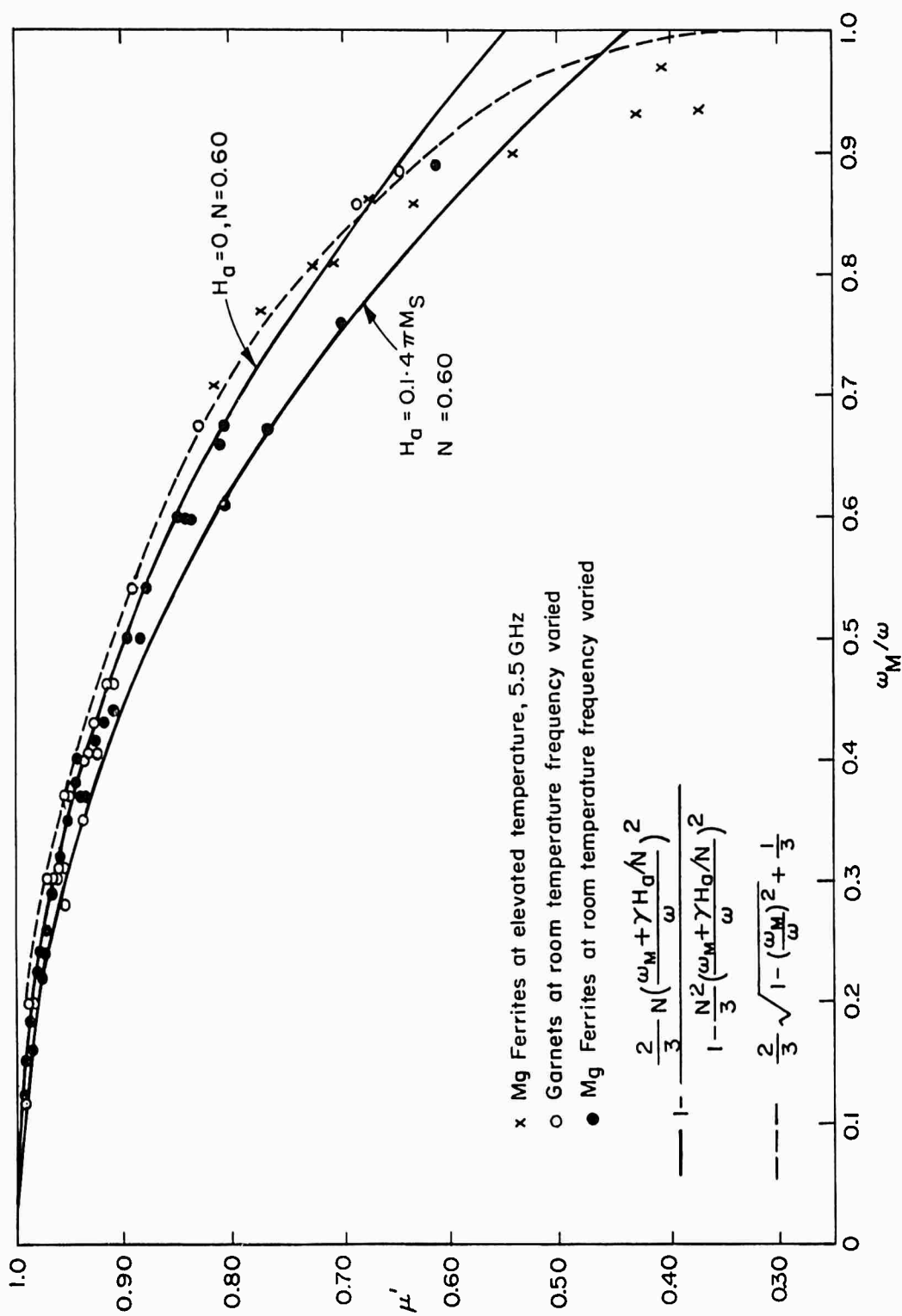


Fig. 2 μ' vs ω_M/ω at $4\pi M = 0$ for Various Garnets and Mg Ferrites

with $N = 0.60$ and $0 < H_a < \frac{1}{10} 4\pi M_s$. Also included in this figure is a theoretical curve of Schlömann for μ' in the demagnetized state vs ω_M/ω

$$\mu' = \frac{2}{3} \sqrt{1 - (\omega_M/\omega^2)} + \frac{1}{3} \quad (7)$$

The derivation of this equation is also given in Appendix II of this report.

SECTION III

THE HIGH POWER PROPERTIES OF PARTIALLY MAGNETIZED MATERIALS

The same materials whose properties have been reported in the previous permeability section are also being measured at high power levels. The program calls for parallel pump measurements at frequencies of 3.0, 5.5, 9.2, and 16.5 GHz at dc fields of 0, $4\pi M_s/3$, and H_{\min} , where H_{\min} is the dc field for the minimum parallel pump threshold (butterfly minimum).⁴ Spherical samples and cavity perturbation techniques are used. For spherical samples $H_{dc} = 0$ corresponds to complete demagnetization and $H_{dc} = 4\pi M_s/3$ corresponds to complete magnetization with an internal dc field approximately equal to zero. Measurements have been completed at 5.5 and 9.2 GHz. The results are summarized in Tables II and III. The tables include the spinwave linewidth ΔH_k computed for $H_{dc} = 4\pi M/3$ and H_{\min} using the parallel pump threshold equation⁴

$$h_{\text{crit}} = \frac{\omega}{\omega_M} \Delta H_k$$

where ω is the signal frequency and $\omega_M = \gamma 4\pi M_s$ with $\gamma = 2\pi$ times the gyro-magnetic ratio. In order to compare the strength of the relaxation mechanism responsible for low power insertion loss with that responsible for the high power threshold the effective linewidth, ΔH_{eff} described in the previous section, is included in the table. ΔH_{eff} was computed for the same signal frequency as the parallel pump threshold experiment was performed.

The following observations can be made on the data presented in Tables II and III. The YIG (G113) and the YAlIG (G810, G1210) have the lowest ΔH_k and ΔH_{eff} among the garnets. The addition of Gd, YGDAlIG (G800, G1200), YGdIG (G1005, G1001) causes a significant increase of ΔH_k and ΔH_{eff} . The MgMnFe (TT1-390) and the MgMnAlFe (TT1-414, TT1-109, and TT1-105) are all quite similar in their ΔH_k and ΔH_{eff} . For those materials which contain Gd, ΔH_{eff} is as much as factor of two larger than ΔH_k . This is due to the frequency dependence⁵ of the rare-earth relaxation mechanism

TABLE II
PARALLEL PUMP - 5.5 GHz

<u>Material</u>	<u>$4\pi M_s$</u>	<u>h_{crit}</u>			<u>ΔH_k</u>		<u>ΔH_{eff}</u>
		<u>Min</u>	<u>$4\pi M_s/3$</u>	<u>0</u>	<u>Min</u>	<u>$4\pi M_s/3$</u>	
G-810	800	2.4	3.9	5.2	1.0	1.6	0.7
G-1210	1200	4.8	6.3	10.4	2.9	3.9	2.5
G-113	1780	2.1	3.0	3.7	1.9	2.7	2.9
G-800	800	14.0	21.0	27.0	5.7	8.6	16.
G-1200	1200	9.3	12.3	18.1	5.7	7.5	13.
G-1005	725	35.0	59.0	>70.0	12.9	21.8	43.
G-1001	1200	12.5	15.5	18.8	7.6	9.5	20.
TT1-414	750	15.3	26.0	33.5	5.8	9.9	13.
TT1-109	1300	5.3	7.8	9.0	3.5	5.2	11.
TT1-105	1750	4.4	6.0	5.4	3.9	5.4	9.
TT1-390	2150	3.7	3.5	---	4.1	3.8	11.

TABLE III
PARALLEL PUMP - 9.2 GHz

Material	$4\pi M_s$	h_{crit}			ΔH_k		ΔH_{eff}
		Min	$4\pi M_s/3$	0	Min	$4\pi M_s/3$	
G-810	800	6.5	11.0	---	1.6	2.7	0.5
G-1210	1200	9.0	15.5	22.2	3.3	5.7	2.0
G-113	1780	4.2	6.9	11.0	2.3	3.7	2.2
G-800	800	37.2	58.9	---	9.1	14.3	17.
G-1200	1200	23.2	29.2	51.3	8.5	10.7	13.
G-1005	725	83.2	---	---	18.4	---	62.
G-1001	1200	27.9	41.7	57.6	10.2	15.2	21.
TT1-414	750	86.2	---	---	19.7	---	16.
TT1-109	1300	13.0	21.1	26.0	5.1	8.4	12.
TT1-105	1750	8.5	12.3	16.6	4.5	6.6	9.
TT1-390	2150	4.8	6.0	8.2	3.2	3.9	10.

(i.e., the spinwave is excited at $\omega/2$, and the uniform precession is excited at ω). The YIG and YAlIG are the lowest loss materials available. The fact that this particular specimen of G810 had the lowest threshold, lower than that of the G113, is an example of microstructural effects (e.g., values of ΔH_k as low as 0.7 Oe have been seen on some Raytheon YIG). Therefore it must be emphasized that the values of ΔH_k and ΔH_{eff} appearing in these tables are neither upper or lower limits, but rather typical values for materials obtained from a commercial supplier. A change of microstructure by an alteration of the material processing procedure will give different values of ΔH_k and ΔH_{eff} . The difference in ΔH_k for $H_{dc} = 4\pi M/3$ and H_{min} is due to a wavelength dependence in ΔH_k .

A desirable feature is low insertion loss and high peak power threshold or, in terms of the relaxation mechanisms, $\Delta H_k \gg \Delta H_{eff}$. In the case of the YAlIG at least, $\Delta H_k > \Delta H_{eff}$. For the gadolinium materials and the spinels $\Delta H_{eff} > \Delta H_k$. From rare-earth relaxation theory one expects $\Delta H_{eff}(\omega) = 2\Delta H_k(\omega/2)$ because of the frequency dependence. Since no theory exists which accounts for the microstructural effects the only comments which can be made are that the microstructure of these particular YAlIG samples has a stronger effect on ΔH_k than on ΔH_{eff} , while on these particular MgMnAlFe samples the opposite is true. The relation between ΔH_k and ΔH_{eff} for those samples containing gadolinium is what would be expected from rare-earth relaxation theory.

REFERENCES

1. "Microwave Properties of Partially Magnetized Ferrites," Final Report RADC-TR-68-312, Raytheon Company, S-1092 (August 1968).
2. R. I. Joseph and E. Schlömann, J. Appl. Phys. 38, 1915 (1967).
3. G. Rado, Phys. Rev. 89, 529 (1953); IRE Trans. AD-4, 512 (1956).
4. E. Schlömann, J. J. Green, and U. Milano, J. Appl. Phys. 31, 386S (1960).
5. J. H. Van Vleck, J. Appl. Phys. 35, 882 (1964).

PERMEABILITY OF PARTIALLY MAGNETIZED FERRITES

Frank Sandy
Raytheon Company
Research Division
Waltham, Massachusetts

ABSTRACT

Existing theories of the partially magnetized state incorrectly predict that $\mu' = \mu'_z = 1.0$. This arises from their neglect of the spatially fluctuating internal rf magnetic field produced by rf magnetic poles on domain and grain boundaries. This report attempts to take these fields into account in a statistical manner. Although the model used is quite crude the theory gives good agreement for μ' and μ'_z vs ω_m/ω in the demagnetized state, qualitatively predicts their dependence on $4\pi M$, and correctly predicts hysteresis in permeability vs $4\pi M$. It fails however to yield a significantly better approximation to κ' vs $4\pi M$ than the earlier theories.

I. INTRODUCTION

Existing theories^{1, 2} of the real part of the permeability of partially magnetized ferrites give

$$\begin{aligned}\mu' &= 1 \\ \mu'_z &= 1 \\ \kappa' &= \gamma 4\pi M/\omega\end{aligned}\tag{1}$$

The equation of κ' is qualitatively correct but the equations for μ' and μ'_z are not, because the derivations do not properly take into account the internal rf magnetic fields produced by rf poles on domain boundaries. These fields are spatially fluctuating and average to zero over the whole sample but still contribute to the permeability of the material. When $\omega_M/\omega > 1$, Polder and Smit³ showed that the effect of these fields was far from negligible and was in fact the source of what is known as low field loss. In the region $\omega_M/\omega < 1$, the effect of these fields is not as spectacular but is still responsible for the errors in Eq. (1).

A proper statistical analysis of these spatially fluctuating internal fields is not available at this time. It is the purpose of this article to show by means of an oversimplified model how these fields affect the permeability. The numeric results however do not fit the data perfectly indicating the necessity to develop a more sophisticated model of a partially magnetized ferrite. However, they do show most of the qualitative features of the dependence of μ' , μ'_z , and κ' on $\gamma 4\pi M/\omega$ and $\gamma 4\pi M_s/\omega$.

II. NOTATION

Before describing the physical model, it is necessary to discuss the notation that will be used to describe the various components of magnetization and magnetic field. The notation and approach are similar to that of Rado.¹ We let \vec{H}_T be the total internal magnetic field at any point in the sample.

$$\bar{H}_T = \bar{H} + \bar{h} \quad (2)$$

where \bar{H} is the dc component of \bar{H}_T and \bar{h} is its rf component. \bar{H} consists of an applied magnetic field less dc demagnetizing fields from the surface, anisotropy fields, and demagnetizing fields from dc poles on domain boundaries. It is often assumed that

$$H \ll 4\pi M_S \quad (3)$$

where $4\pi M_S$ is the saturation induction of the material. The total magnetization \bar{M}_T of the sample is composed of a dc part \bar{M}_S and a small rf component \bar{m} . We can write

$$\bar{M}_T = \bar{M}_S + \bar{m} \quad (4)$$

where the magnitudes of \bar{M}_S and \bar{M}_T are equal since we are dealing only with the low power limit. Each of the quantities \bar{H} , \bar{M}_S , and \bar{h} can then be divided into an average part denoted by brackets $\langle \rangle$ and a spatially fluctuating part denoted by δ .

$$\begin{aligned} \bar{H} &= \langle \bar{H} \rangle + \delta \bar{H} \\ \bar{h} &= \langle \bar{h} \rangle + \delta \bar{h} \\ \bar{m} &= \langle \bar{m} \rangle + \delta \bar{m} \\ \bar{M}_S &= \langle \bar{M}_S \rangle + \delta \bar{M} \end{aligned} \quad (5)$$

We shall also denote the average or measured magnetization $\langle \bar{M}_S \rangle$ by its usual symbol, \bar{M} . The average internal magnetic field $\langle \bar{h} \rangle$ is just the applied rf magnetic field less the rf demagnetizing field from the sample boundary. The permeability tensor $\bar{\mu}$

$$\bar{\mu} = \begin{pmatrix} \mu & -jk & 0 \\ jk & \mu & 0 \\ 0 & 0 & \mu_z \end{pmatrix}, \quad (6)$$

which we are trying to find, is defined by

$$4\pi \langle \overline{m} \rangle = (\overline{\mu} - 1) \cdot \langle \overline{h} \rangle \quad (7)$$

III. THEORY

We shall obtain $\overline{\mu}$ by starting from the torque equation.

$$\overline{M}_T = j\omega \overline{m} = -\gamma (\overline{M}_T \times \overline{H}_T) \quad (8)$$

where

$$\gamma = \frac{g|e|}{2mc} \quad (9)$$

By incorporating Eqs. (2), (4), and (5) into (8) making use of the approximation in Eq. (3) and neglecting terms quadric in the rf fields, we obtain

$$\langle \overline{m} \rangle + \delta \overline{m} = -\frac{\gamma}{j\omega} \{ \langle \overline{M}_S \rangle \times \langle \overline{h} \rangle + \langle \overline{M}_S \rangle \times \delta \overline{h} + \delta \overline{M} \times \langle \overline{h} \rangle + \delta \overline{M} \times \delta \overline{h} \} \quad (10)$$

Taking the spatial average of Eq. (10) and noting that by definition

$$\langle \delta \overline{m} \rangle = \langle \delta \overline{h} \rangle = \langle \delta \overline{M} \rangle = 0 \quad (11)$$

we get

$$\begin{aligned} \langle \overline{m} \rangle &= \frac{-\gamma}{j\omega} \{ \langle \overline{M}_S \rangle \times \langle \overline{h} \rangle + \langle \delta \overline{M} \times \delta \overline{h} \rangle \} \\ &= \frac{-\gamma}{j\omega} \{ \overline{M} \times \langle \overline{h} \rangle + \langle \delta \overline{M} \times \delta \overline{h} \rangle \} \end{aligned} \quad (12)$$

At this point Rado asserts that $\delta \overline{M}$ and $\delta \overline{h}$ are uncorrelated so that

$$\langle \delta \overline{M} \times \delta \overline{h} \rangle = \langle \delta \overline{M} \rangle \times \langle \delta \overline{h} \rangle = 0$$

and hence

$$\overline{m} = -\frac{\gamma}{j\omega} \overline{M} \times \langle \overline{h} \rangle \quad (14)$$

If we let \overline{M} be in the \hat{z} direction and let $\langle \overline{h} \rangle$ be in the \hat{x}, \hat{z} plane (where \hat{x} and \hat{z} are unit vectors), then

$$\begin{aligned} m_x &= 0 \\ m_y &= j \frac{\gamma M}{\omega} \langle h_x \rangle \\ m_z &= 0 \end{aligned} \quad (15)$$

From this, one obtains Eqs. (1). Unfortunately $\delta \overline{M}$ and $\delta \overline{h}$ are correlated and Eq. (13) is not valid. To see why $\delta \overline{M}$ and $\delta \overline{h}$ are correlated, we must consider a model that gives us more information about the relationship of $\delta \overline{M}$ to $\delta \overline{h}$.

IV. MODEL

We shall assume that each domain is ellipsoidal with a demagnetizing tensor $\overline{\overline{N}}$. We will then have a contribution to $\delta \overline{h}$ from the rf poles on its own domain boundary. We will denote this by $\delta \overline{h}_1$:

$$\begin{aligned} \delta \overline{h}_1 &= -\overline{\overline{N}} \cdot (\overline{m} - \overline{m}_1) = -\overline{\overline{N}} \cdot (\overline{m} - \langle \overline{m} \rangle + \delta \overline{m}_1) \\ &= -\overline{\overline{N}} \cdot \delta \overline{m} + \overline{\overline{N}} \cdot \delta \overline{m}_1 \end{aligned} \quad (16)$$

where \overline{m}_1 is the rf magnetization of the material surrounding the given domain. We shall assume that $\delta \overline{m}_1$, the deviation of \overline{m}_1 from $\langle \overline{m} \rangle$ is uncorrelated with the $\delta \overline{M}$ of the domain in question. We will also assume that the contributions to $\delta \overline{h}$ from poles on all other domain walls other than that surrounding the domain in question are uncorrelated with $\delta \overline{M}$. Thus we will write

$$\delta \bar{h} = - \bar{N} \cdot \delta \bar{m} + \text{terms uncorrelated with } \delta \bar{m}. \quad (17)$$

Since we will be concerned only with $\langle \delta \bar{M} \times \delta \bar{h} \rangle$, we shall neglect all terms uncorrelated with $\delta \bar{M}$ at this time. Thus we have

$$\delta \bar{h} = - \bar{N} \cdot \delta \bar{m} \quad (18)$$

We further assume without any justification that the deviation of \bar{N} from its average is uncorrelated with $\delta \bar{M}$. This approximation is the primary reason for what disagreement there will be between theory and experiment. However, these approximations are necessary to make the mathematics tractable. We thus have as the approximation to be used in our model

$$\delta \bar{h} = - 4\pi N \delta \bar{m} \quad (19)$$

where N is an average scalar value of the demagnetizing factor. Although this has the appearance of asserting that $\delta \bar{h}$ is related to $\delta \bar{m}$ by a point relationship, which would be quite dubious, it is only being assumed that that part of $\delta \bar{h}$ which is correlated to $\delta \bar{M}$ is related to $\delta \bar{m}$ by such a point relationship.

Before evaluating $\langle \delta \bar{M} \times \delta \bar{h} \rangle$ explicitly, it is worthwhile to demonstrate qualitatively for the simple case where $4\pi M = 0$ just why $\langle \delta \bar{M} \times \delta \bar{h} \rangle$ is not zero. Rado's argument that it is zero states that for any domain with a given $\delta \bar{M}$ and $\delta \bar{h}$ there is another domain with equal probability having the same $\delta \bar{h}$ and opposite $\delta \bar{M}$. But let us see what actually happens when we reverse $\delta \bar{M}$ of one domain keeping everything else constant. Since $4\pi M = 0$, each $\delta \bar{M}$ has the magnitude of M_s and the rf magnetization of each domain precesses about the direction of $\delta \bar{M}$. If we reverse the direction of $\delta \bar{M}$, we reverse the direction of precession of the magnetization and also the direction of precession of the $\delta \bar{h}$ induced by the magnetization. The components of $\delta \bar{h}$ parallel to the drive field are equal for these two oppositely magnetized domains and the components of $\delta \bar{h}$ perpendicular to the drive field and to $\delta \bar{M}$

will be opposite in sign. Thus the components of $\delta\bar{M} \times \delta\bar{h}$ parallel to the applied field will add and only the components perpendicular to the drive field and $\delta\bar{M}$ will cancel each other. Thus $\langle \delta\bar{M} \times \delta\bar{h} \rangle$ has a component parallel to the drive field yielding a contribution to μ' and μ'_z not predicted by Rado.

V. EVALUATION OF $\langle \delta\bar{M} \times \delta\bar{h} \rangle$

We can now proceed to evaluate $\langle \delta\bar{M} \times \delta\bar{h} \rangle$ in terms of our model. We first rewrite Eq. (10) including the terms in $\langle \bar{H} \rangle$ and $\delta\bar{H}$ which were neglected but noting that $\bar{M}_s \times \bar{H} = 0$.

$$\begin{aligned} \langle \bar{m} \rangle + \delta\bar{m} = & -\frac{\gamma}{j\omega} \{ \bar{M} \times \langle \bar{h} \rangle + \bar{M} \times \delta\bar{h} + \delta\bar{M} \times \langle \bar{h} \rangle + \delta\bar{M} \times \delta\bar{h} \\ & + \langle \bar{m} \rangle \times \langle \bar{H} \rangle + \langle \bar{m} \rangle \times \delta\bar{H} + \delta\bar{m} \times \langle \bar{H} \rangle + \delta\bar{m} \times \delta\bar{H} \} \end{aligned} \quad (20)$$

Taking the spatial average of both side as before

$$\langle \bar{m} \rangle = -\frac{\gamma}{j\omega} \{ \bar{M} \times \langle \bar{h} \rangle - \langle \bar{H} \rangle \times \langle \bar{m} \rangle + \langle \delta\bar{M} \times \delta\bar{h} \rangle - \langle \delta\bar{H} \times \delta\bar{m} \rangle \} \quad (21)$$

Making use of our basic assumption, Eq. (19), we can rewrite this as

$$\langle \bar{m} \rangle = -\frac{\gamma}{j\omega} \{ \bar{M} \times \langle \bar{h} \rangle - \langle \bar{H} \rangle \times \langle \bar{m} \rangle + \langle (\delta\bar{M} + \frac{\delta\bar{H}}{N}) \times \delta\bar{h} \rangle \} \quad (22)$$

Equation (22) has two additional terms that were absent from Eq. (12). The term in $\langle \bar{H} \rangle \times \langle \bar{m} \rangle$ states that when the material approaches saturation and the spatially fluctuating terms $\delta\bar{M}$ and $\delta\bar{h}$ go to zero, the sample behaves as if it were in a dc field of $\langle \bar{H} \rangle$. In this case, however, $\langle \bar{H} \rangle$ is not primarily an applied dc field but rather an average of anisotropy and other internal fields. For $|\gamma \langle \bar{H} \rangle| \equiv \omega_0 \ll \omega$ this term contributes an amount $-\omega_0 \omega_M / \omega^2$ to μ' but makes no contribution to κ' or μ'_z . The next

additional term $\delta H/N \times \delta h$ has an effect similar to $\delta M \times \delta h$ only smaller. Since it greatly complicates the calculations without making a substantial contribution, we shall calculate $\langle \delta \bar{M} \times \delta \bar{h} \rangle$ assuming $\bar{H} = 0$ and replace $\delta \bar{M}$ in the final result by $\delta \bar{M} + \delta \bar{H}/N$. With $\bar{H} = 0$ subtracting Eq. (21) from Eq. (20) yields

$$\delta \bar{m} = -\frac{\gamma}{j\omega} \{ \bar{M} \times \delta \bar{h} + \delta \bar{M} \times \langle \bar{h} \rangle + \delta \bar{M} \times \delta \bar{h} - \langle \delta \bar{M} \times \delta \bar{h} \rangle \}. \quad (23)$$

Combining the first and third terms of Eq. (23) and making use of Eq. (19) we get

$$\delta \bar{h} = \frac{4\pi\gamma N}{j\omega} \{ \bar{M}_s \times \delta \bar{h} + \delta \bar{M} \times \langle \bar{h} \rangle - \langle \delta \bar{M} \times \delta \bar{h} \rangle \} \quad (24)$$

We must now solve this equation for $\langle \delta \bar{M} \times \delta \bar{h} \rangle$ in terms of $4\pi\gamma \bar{M}_s/\omega$, $\gamma \langle \bar{H} \rangle/\omega$, $\langle \bar{h} \rangle$, N , and the statistics of $\delta \bar{M}$. Having done this, the result can be substituted into Eq. (22) and the components of $\langle \bar{m} \rangle$ found as a function of the components of $\langle \bar{h} \rangle$. The details of this algebra and the mathematical approximations necessary are described in the appendix. The results of this calculations are

$$\mu' - 1 \approx \frac{-\left(\frac{4\pi\gamma}{\omega}\right)^2 N (\langle \delta M^2 \rangle - \langle \delta M_x^2 \rangle)}{\left\{ 1 - \left(\frac{4\pi\gamma}{\omega}\right)^2 N^2 (M^2 + \langle \delta M_x^2 \rangle) \right\}} - \frac{4\pi\gamma^2}{\omega^2} M \langle H \rangle \quad (25a)$$

$$\mu'_z - 1 \approx \frac{-\left(\frac{4\pi\gamma}{\omega}\right)^2 N (\langle \delta M^2 \rangle - \langle \delta M_z^2 \rangle)}{\left\{ 1 - \left(\frac{4\pi\gamma}{\omega}\right)^2 N^2 (M^2 + \langle \delta M_z^2 \rangle) \right\}} \quad (25b)$$

$$\kappa' \approx \frac{4\pi\gamma}{\omega} M - \frac{\left(\frac{4\pi\gamma}{\omega}\right)^3 \{ N^2 M \langle \delta M_z^2 \rangle - \frac{N}{4\pi} \langle H \rangle (\langle \delta M^2 \rangle - \langle \delta M_x^2 \rangle) \}}{\left\{ 1 - \left(\frac{4\pi\gamma}{\omega}\right)^2 N^2 (M^2 + \langle \delta M_x^2 \rangle) \right\}} \quad (25c)$$

where

$$\langle \delta M^2 \rangle = \langle \delta M_x^2 \rangle + \langle \delta M_y^2 \rangle + \langle \delta M_z^2 \rangle \quad (26)$$

and

$$\langle \delta M_x^2 \rangle = \langle \delta M_y^2 \rangle \quad (27)$$

Since

$$\overline{M}_s = \overline{M} + \delta \overline{M} \quad (28)$$

We have by squaring and averaging

$$M_s^2 = M^2 + \langle \delta M^2 \rangle \quad (29)$$

or

$$\langle \delta M^2 \rangle = M_s^2 - M^2 \quad (30)$$

When the material is isotropically demagnetized

$$\langle \delta M_x^2 \rangle = \langle \delta M_z^2 \rangle = \frac{1}{3} \langle \delta M^2 \rangle = \frac{1}{3} M_s^2 \quad (31)$$

and

$$\mu' - 1 = \mu'_z - 1 = -\frac{2}{3} N \frac{(\omega_M/\omega)^2}{1 - \frac{N^2}{3} (\omega_M/\omega)^2} \quad (32)$$

In order to qualitatively take into account the anisotropy and other internal fields that were dropped from Eq. (22), we indicated we would replace $\delta \overline{M}$ by $\delta \overline{M} + \delta \overline{H}/N$ in our final results. In an isotropically demagnetized material $\langle \overline{H} \rangle$ is also zero. Thus $\delta \overline{H}$ is parallel to $\delta \overline{M}$. If we define H_a as $\langle |\delta H| \rangle$, Eq. (32) then becomes

$$\mu' - 1 = \mu'_z = -\frac{2}{3}N \frac{(\omega_M + \gamma H_a/N)^2/\omega^2}{1 - \frac{N^2}{3}(\omega_M + \gamma H_a/N)^2/\omega^2} \quad (33)$$

VI. COMPARISON WITH EXPERIMENT

The next question to be considered is the value of N . If our domains were surrounded by nonmagnetic material the sum of the three diagonal components of \bar{N} would be 1.0 and the average value, N , would be one third. However, Polder and Smit³ have shown that for some domain configurations the sum of the diagonal components of \bar{N} can be 2.0. Thus we must use an experimentally determined value. In Fig. 1, we have μ' plotted vs ω_M/ω for several materials and frequencies. The field H_a , a combination of anisotropy and demagnetizing fields, is not well known, but is much less than $4\pi M_s$. We have also plotted Eq. (33) for $H_a = 0$ and $4\pi M_s/10$ with $N = 0.60$. This value of N gives the best fit for these values of H_a . With larger values of H_a , a smaller value of N would be required.

We thus see that the theory gives reasonable agreement with the experimental results for μ' vs ω_M/ω in the demagnetized state. We shall now examine how well Eqs. (25) describe the dependence of μ' , μ'_z , and κ' on $4\pi M$ as one cycles about the B-H hysteresis loop. First one should note that the expressions for these components of the permeability tensor depend on $\langle \delta M^2 \rangle$, $\langle \delta M_x^2 \rangle$, and $\langle \delta M_z^2 \rangle$. In Eq. (30) we showed that $\langle \delta M^2 \rangle$ is a unique function of M and M_s . However, its components are not unique functions of M and M_s and depend in addition on the specific domain geometry and hence on hysteresis history. Thus the permeability shows hysteresis as a function of $4\pi M$. Two states having the same magnetization but on opposite sides of the B-H hysteresis loop have different permeability. This hysteresis is observed experimentally.⁴ Its magnitude and even sign vary from material to material. Without a better understanding of domain dynamics in polycrystalline materials, a theoretical description of how $\langle \delta M_x^2 \rangle$ and $\langle \delta M_z^2 \rangle$ vary around the hysteresis loop is not possible.

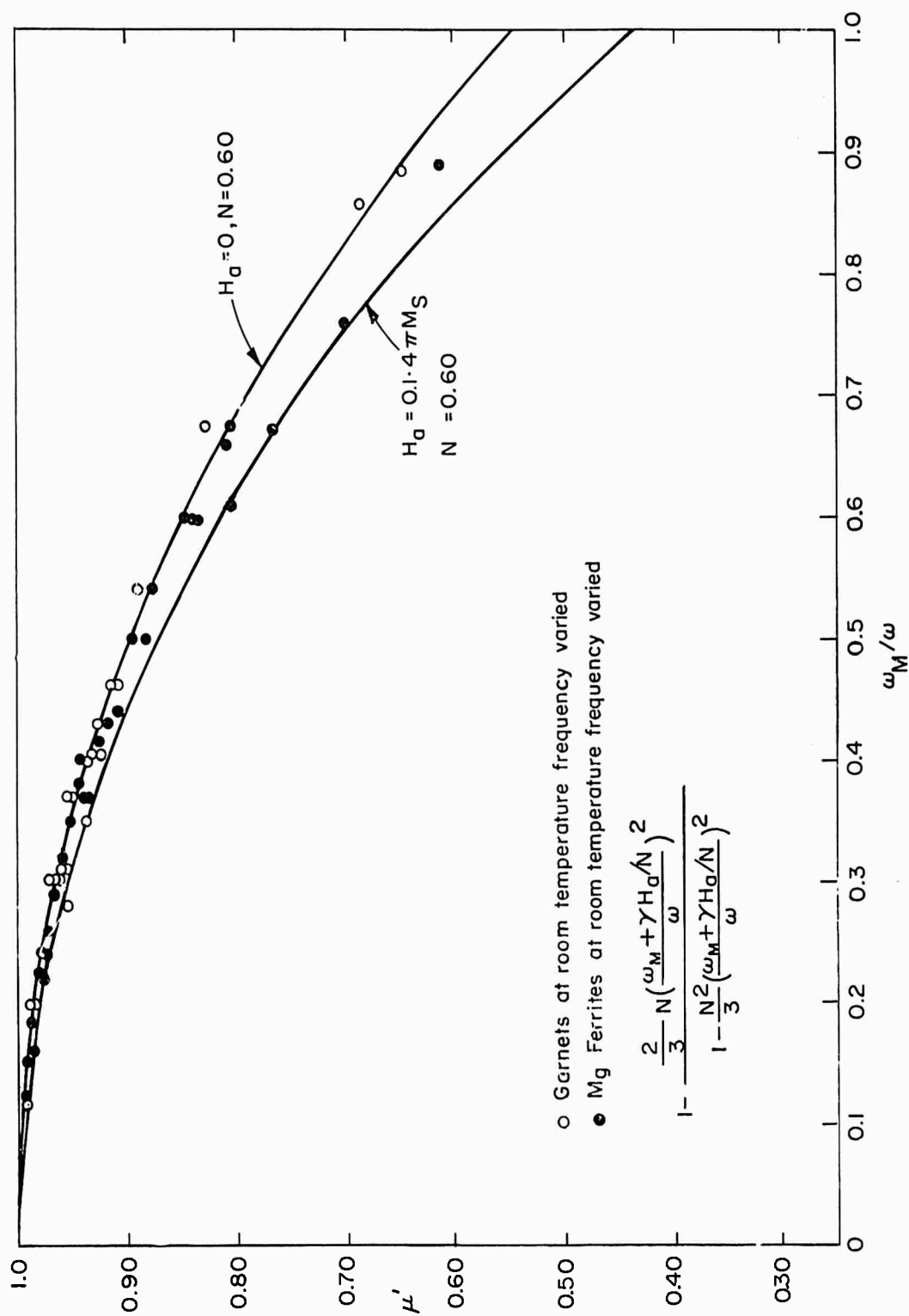


Fig. 1 μ' vs ω_M/ω in the Demagnetized State

We next note the difference in behavior of μ' and μ'_z as a function of $4\pi M$. The prime difference is the term $M\langle\bar{H}\rangle$ in μ' . At applied dc fields several times the coercive force $4\pi M$ is still well below saturation but is as large as it can be made without making the applied dc field very large. Since $\langle\delta M^2\rangle$ does not go to zero until $4\pi M = 4\pi M_s$, μ' and μ'_z do not equal 1.0 at this point. However, μ'_z is approaching 1.0 as $4\pi M \rightarrow 4\pi M_s$ and $\langle\delta M^2\rangle \rightarrow 0$. This follows from Eq. (25b) and is observed experimentally.⁴ On the other hand μ' is observed not to approach 1.0 as $4\pi M \rightarrow 4\pi M_s$ but rather flattens out and eventually turns downward. Earlier explanations⁴ attributed this to the contribution of the applied dc field to the permeability. This is only part of the explanation. The actual source of this roll off in μ' vs $4\pi M$ is the term $M\langle\bar{H}\rangle$. While the applied dc field contributes to $\langle\bar{H}\rangle$, the major contribution to this term is anisotropy and dc demagnetizing fields. It should be noted that $\langle\bar{H}\rangle$ the average internal effective dc field taken near saturation and $H_a = \langle|\delta H|\rangle$, the average magnitude of this internal effective dc field taken in the demagnetized state are related quantities but not necessarily identical.

To understand in detail how $\langle\bar{H}\rangle$ and $\langle|\delta H|\rangle$ depend on anisotropy and porosity, it is necessary to have a better understanding of domain structure than is presently available. However, it can be seen that \bar{H} is a measure of how tightly each domain is bound to its equilibrium orientation. Increasing porosity puts additional constraints on the domain formation, binding the domains more closely to their equilibrium position and increasing $\langle\bar{H}\rangle$ for partially magnetized states. As a result μ' will not come as close to 1.0 for a porous materials as a dense one with the same magnetization and anisotropy. It is observed experimentally that microwave phase shifters, such as PIP,⁵ that depend on the change in μ' from the demagnetized state to that at B-H loop closure for their phase shift, lose phase shift rapidly with small amounts of porosity. This tends to confirm the previous argument. However, the argument can be rephrased to predict the $H_a = \langle|\delta \bar{H}|\rangle$ also increases with porosity and hence $|\mu' - 1|$ is greater for porous materials than dense materials when $4\pi M = 0$. This has not been observed, and might be due to

the fact that the demagnetized state is more random and hence the porosity may have less effect in "stiffening" the domain pattern than in the more ordered state near B-H loop closure.

The remaining prediction of this theory to be examined is the dependence of κ' on $4\pi M$. The leading term of Eq. (26c) is the same as Rado's result as is expected. The corrections include terms containing $\langle \delta M_x^2 \rangle$ and $\langle \delta M_z^2 \rangle$ and hence hysteresis in κ' vs $4\pi M$ is predicted. This is observed experimentally. However, the theory has this hysteresis going to zero when $4\pi M = 0$, and this is contradicted by experiment.⁴ It is at this point that the deficiencies of the model become apparent. The terms in $\delta \bar{h}$ which we neglected as uncorrelated to $\delta \bar{M}$ do have a measurable effect although small compared to the other effects predicted by the theory. In particular by ignoring the correlation between \bar{N} and the direction of $\delta \bar{M}$ we lost information that differentiates the two states with $4\pi M = 0$ and applied field equal to \pm the coercive force.

VII. SUMMARY

The theory presented here predicts the following phenomena which are experimentally observed:

1. μ' and μ'_z differ from 1.0 in partially magnetized states,
2. A formula is given for the dependence of μ' and μ'_z in the demagnetized state on ω_M/ω which is quantitatively correct for $\omega_M/\omega < 0.9$,
3. Hysteresis in μ' , μ'_z , and κ' vs $4\pi M$ is to be expected. The theory allows for hysteresis of either sign and does not predict its magnitude,
4. μ'_z approaches 1.0 as the material saturates,
5. μ' does not approach 1.0 as the material saturates and remains below it by an amount given by an effective internal dc field made up of anisotropy, demagnetizing, and the applied field.

The theory also predicts that hysteresis in κ' goes to zero as $4\pi M$ goes to zero. This is contradicted by experiment.

REFERENCES TO APPENDIX I

1. G. Rado, Phys. Rev. 89, 529, IRE Trans. AD-4, 512 (1956).
2. R. F. Soohoo, IRE Convention Record, Pt V. 84 (1956).
3. D. Polder and J. Smit, Rev. Mod. Phys. 25, 89 (1953).
4. "Microwave Properties of Partially Magnetized Ferrites," Final Report RADC-TR-68-312, Raytheon Research Division Report S-1092 (August 1968).
5. "Study of PIP, the Ku-Band Polarization Sensitive Phase Shifter," J. J. Green, M. R. Harris, E. A. Maguire, and F. Sandy, Raytheon Technical Memorandum T-735 (1967).

APPENDIX I-A

This appendix contains the algebra necessary to obtain the permeability tensor components as given in Eq. (25) from the formula for $\delta\bar{h}$ given in Eq. (27).

As a notational convention $\bar{A} \times \bar{B} \times \bar{C}$ will mean $\bar{A} \times (\bar{B} \times \bar{C})$. We make use of the following vector identities:

$$\bar{A} \times \bar{B} \times \bar{C} = \bar{B}(\bar{A} \cdot \bar{C}) - \bar{C}(\bar{A} \cdot \bar{B}) \quad (A1)$$

$$\bar{A} \cdot \bar{B} \times \bar{B} = 0 \quad (A2)$$

and the definitions

$$\bar{M}_s = \bar{M} + \delta\bar{M} \quad (A3)$$

$$\langle \delta M^2 \rangle = \langle \delta M_x^2 \rangle + \langle \delta M_y^2 \rangle + \langle \delta M_z^2 \rangle \quad (A4)$$

and the symmetry condition

$$\langle \delta M_x^2 \rangle = \langle \delta M_y^2 \rangle \quad (A5)$$

We begin by twice taking the cross product from the left of Eq. (24) with \bar{M}_s .

$$\bar{M}_s \times \delta\bar{h} = \left(\frac{4\pi\gamma N}{j\omega}\right) \{ \bar{M}_s \times \delta\bar{M} \times \langle \bar{h} \rangle + \bar{M}_s \times \bar{M}_s \times \delta\bar{h} - \bar{M}_s \times \langle \delta\bar{M} \times \delta\bar{h} \rangle \} \quad (A6)$$

$$\begin{aligned} \bar{M}_s \times \bar{M}_s \times \delta\bar{h} = & \left(\frac{4\pi\gamma N}{j\omega}\right) \{ \bar{M}_s \times \bar{M}_s \times \delta\bar{M} \times \langle \bar{h} \rangle + \bar{M}_s \times \bar{M}_s \times \delta\bar{h} - \bar{M}_s \times \bar{M}_s \\ & \times \langle \delta\bar{M} \times \delta\bar{h} \rangle \} \quad (A7) \end{aligned}$$

Making use of Eqs. (A1), (A2), and (A3), Eq. (A7) becomes

$$\begin{aligned} \overline{\mathbf{M}}_s \times \overline{\mathbf{M}}_s \times \delta \mathbf{h} = \frac{4\pi\gamma N}{j\omega} \{ & - \overline{\mathbf{M}}_s \overline{\mathbf{M}}_s \cdot (\overline{\mathbf{M}} \times \langle \mathbf{h} \rangle) - M_s^2 (\delta \overline{\mathbf{M}} \times \langle \mathbf{h} \rangle) - M_s^2 (\overline{\mathbf{M}}_s \times \delta \mathbf{h}) \\ & - \overline{\mathbf{M}}_s \overline{\mathbf{M}}_s \cdot \langle \delta \overline{\mathbf{M}} \times \delta \mathbf{h} \rangle + M_s^2 \langle \delta \overline{\mathbf{M}} \times \delta \mathbf{h} \rangle \} \quad . \quad (\text{A8}) \end{aligned}$$

Substituting Eq. (A8) into Eq. (A6)

$$\begin{aligned} \overline{\mathbf{M}}_s \times \delta \mathbf{h} = \frac{4\pi\gamma N}{j\omega} [& \overline{\mathbf{M}}_s \times \delta \overline{\mathbf{M}} \times \langle \mathbf{h} \rangle + \frac{4\pi\gamma N}{j\omega} \{ - \overline{\mathbf{M}}_s \overline{\mathbf{M}}_s \cdot (\overline{\mathbf{M}} \times \langle \mathbf{h} \rangle) - M_s^2 (\delta \overline{\mathbf{M}} \times \langle \mathbf{h} \rangle) \\ & - M_s^2 (\overline{\mathbf{M}}_s \times \delta \mathbf{h}) - \overline{\mathbf{M}}_s \overline{\mathbf{M}}_s \cdot \langle \delta \overline{\mathbf{M}} \times \delta \mathbf{h} \rangle + M_s^2 \langle \delta \overline{\mathbf{M}} \times \delta \mathbf{h} \rangle \} - \overline{\mathbf{M}}_s \times \langle \delta \overline{\mathbf{M}} \times \delta \mathbf{h} \rangle] . \quad (\text{A9}) \end{aligned}$$

Taking the spatial average of both sides, noting that M_s^2 is a constant gives

$$\begin{aligned} \langle \overline{\mathbf{M}}_s \times \delta \mathbf{h} \rangle = \frac{4\pi\gamma N}{j\omega} [& \langle \overline{\mathbf{M}}_s \times \delta \overline{\mathbf{M}} \times \langle \mathbf{h} \rangle \rangle + \frac{4\pi\gamma N}{j\omega} \{ - \langle \overline{\mathbf{M}}_s \overline{\mathbf{M}}_s \rangle \cdot (\overline{\mathbf{M}} \times \langle \mathbf{h} \rangle) \\ & - M_s^2 \langle \delta \overline{\mathbf{M}} \times \langle \mathbf{h} \rangle \rangle - M_s^2 \langle \overline{\mathbf{M}}_s \times \delta \mathbf{h} \rangle - \langle \overline{\mathbf{M}}_s \overline{\mathbf{M}}_s \rangle \cdot \langle \delta \overline{\mathbf{M}} \times \delta \mathbf{h} \rangle \\ & + M_s^2 \langle \delta \overline{\mathbf{M}} \times \delta \mathbf{h} \rangle \} - \langle \overline{\mathbf{M}}_s \rangle \times \langle \delta \overline{\mathbf{M}} \times \delta \mathbf{h} \rangle] \quad . \quad (\text{A10}) \end{aligned}$$

Using Eq. (A3) and noting that the product of constants and one spatially fluctuating variable has an average of zero, we get, after collecting terms in Eq. (A10)

$$\begin{aligned} \langle \delta \overline{\mathbf{M}} \times \delta \mathbf{h} \rangle = \frac{4\pi\gamma N}{j\omega} [& \langle \delta \overline{\mathbf{M}} \times \delta \overline{\mathbf{M}} \times \langle \mathbf{h} \rangle \rangle + \frac{4\pi\gamma N}{j\omega} \{ - \langle \overline{\mathbf{M}}_s \overline{\mathbf{M}}_s \rangle \cdot (\overline{\mathbf{M}} \times \langle \mathbf{h} \rangle) \\ & - \langle \overline{\mathbf{M}}_s \overline{\mathbf{M}}_s \rangle \cdot \langle \delta \overline{\mathbf{M}} \times \delta \mathbf{h} \rangle \} - \overline{\mathbf{M}} \times \langle \delta \overline{\mathbf{M}} \times \delta \mathbf{h} \rangle] \quad . \quad (\text{A11}) \end{aligned}$$

By symmetry

$$\langle \delta M_x \delta M_y \rangle = \langle \delta M_y \delta M_z \rangle = \langle \delta M_z \delta M_x \rangle = 0 \quad . \quad (\text{A12})$$

Therefore

$$\langle M_s M_s \rangle \cdot \bar{A} = \langle M_{sx}^2 \rangle A_x \hat{x} + \langle M_{sy}^2 \rangle A_y \hat{y} + \langle M_{sz}^2 \rangle A_z \hat{z} \quad (A13)$$

where A is any constant vector,

$$\begin{aligned} \langle M_{sx}^2 \rangle &= \langle \delta M_x^2 \rangle \\ \langle M_{sy}^2 \rangle &= \langle \delta M_y^2 \rangle \\ \langle M_{sz}^2 \rangle &= M^2 + \langle \delta M_z^2 \rangle \end{aligned} \quad (A14)$$

and \hat{x} , \hat{y} , and \hat{z} are unit vectors.

In addition

$$\begin{aligned} \langle \delta \bar{M} \times \delta \bar{M} \times \langle \bar{h} \rangle \rangle &= \langle \delta \bar{M} \delta \bar{M} \rangle \cdot \langle \bar{h} \rangle - \langle \delta M^2 \rangle \langle \bar{h} \rangle \\ &= (\langle \delta M_x^2 \rangle - \langle \delta M^2 \rangle) \langle h_x \rangle + (\langle \delta M_y^2 \rangle - \langle \delta M^2 \rangle) \langle h_y \rangle \hat{y} \\ &\quad + (\langle \delta M_z^2 \rangle - \langle \delta M^2 \rangle) \langle h_z \rangle \hat{z} \end{aligned} \quad (A15)$$

If we write Eq. (A11) in component form, making use of Eqs. (A13) and (A15), we have three simultaneous equations for the three components of $\langle \delta \bar{M} \times \delta \bar{h} \rangle$. Without loss of generality we can again take $\langle \bar{h} \rangle$ to be in the x-z plane so that $\langle h_y \rangle = 0$

$$\begin{aligned} \langle \delta \bar{M} \times \delta \bar{h} \rangle_x &= \frac{4\pi\gamma N}{j\omega} [(\langle \delta M_x^2 \rangle - \langle \delta M^2 \rangle) \langle h_x \rangle + \frac{4\pi\gamma N}{j\omega} \{ -\langle \delta M_x^2 \rangle \langle \delta M \times \delta h_x \rangle \} \\ &\quad + M \langle \delta \bar{M} \times \delta \bar{h} \rangle_y] \\ \langle \delta \bar{M} \times \delta \bar{h} \rangle_y &= \frac{4\pi\gamma N}{j\omega} [\frac{4\pi\gamma N}{j\omega} \{ -\langle \delta M_y^2 \rangle M \langle h_x \rangle - \langle \delta M_y^2 \rangle \langle \delta M \times \delta h \rangle_y \} - M \langle \delta \bar{M} \times \delta \bar{h} \rangle_x] \\ \langle \delta \bar{M} \times \delta \bar{h} \rangle_z &= \frac{4\pi\gamma N}{j\omega} [(\langle \delta M_z^2 \rangle - \langle \delta M^2 \rangle) \langle h_z \rangle + \frac{4\pi\gamma N}{j\omega} \{ - (M^2 + \langle \delta M_z^2 \rangle) \langle \delta \bar{M} \times \delta \bar{h} \rangle_z \}] \end{aligned} \quad (A16)$$

Collecting terms and making use of Eq. (A5) gives

$$\begin{aligned}
\left\{1 + \left(\frac{4\pi\gamma N}{j\omega}\right)^2 \langle \delta M_x^2 \rangle\right\} \langle \delta \bar{M} \times \delta \bar{h} \rangle_x - \left(\frac{4\pi\gamma N}{j\omega}\right) M \langle \delta \bar{M} \times \delta \bar{h} \rangle_y &= \frac{4\pi\gamma N}{j\omega} (\langle \delta M_x^2 \rangle - \langle \delta M^2 \rangle) \langle h_x \rangle \\
\left(\frac{4\pi\gamma N}{j\omega}\right) M \langle \delta \bar{M} \times \delta \bar{h} \rangle_x + \left\{1 + \left(\frac{4\pi\gamma N}{j\omega}\right)^2 \langle \delta M_x^2 \rangle\right\} \langle \delta \bar{M} \times \delta \bar{h} \rangle_y &= -\left(\frac{4\pi\gamma N}{j\omega}\right)^2 \langle \delta M_x^2 \rangle M \langle h_x \rangle \\
\left\{1 + \left(\frac{4\pi\gamma N}{j\omega}\right)^2 (M^2 + \langle \delta M_z^2 \rangle)\right\} \langle \delta \bar{M} \times \delta \bar{h} \rangle_z &= \frac{4\pi\gamma N}{j\omega} (\langle \delta M_z^2 \rangle - \langle \delta M^2 \rangle) \langle h_z \rangle
\end{aligned} \tag{A17}$$

Solving these equations yields

$$\begin{aligned}
\langle \delta \bar{M} \times \delta \bar{h} \rangle_x &= \frac{\left(\frac{4\pi\gamma N}{j\omega}\right) (\langle \delta M_x^2 \rangle - \langle \delta M^2 \rangle) \left(1 + \left(\frac{4\pi\gamma N}{j\omega}\right)^2 \langle \delta M_x^2 \rangle\right) - \left(\frac{4\pi\gamma N}{j\omega}\right)^3 \langle \delta M_x^2 \rangle M^2}{\left\{1 + \left(\frac{4\pi\gamma N}{j\omega}\right)^2 \langle \delta M_x^2 \rangle\right\}^2 + \left(\frac{4\pi\gamma N}{j\omega}\right)^2 M^2} \langle h_x \rangle \\
\langle \delta \bar{M} \times \delta \bar{h} \rangle_y &= \frac{-\left(\frac{4\pi\gamma N}{j\omega}\right)^2 M (2 \langle \delta M_x^2 \rangle - \langle \delta M^2 \rangle) - \left(\frac{4\pi\gamma N}{j\omega}\right)^4 \langle \delta M_x^2 \rangle^2 M}{\left\{1 + \left(\frac{4\pi\gamma N}{j\omega}\right)^2 \langle \delta M_x^2 \rangle\right\}^2 + \left(\frac{4\pi\gamma N}{j\omega}\right)^2 M^2} \langle h_x \rangle \\
\langle \delta \bar{M} \times \delta \bar{h} \rangle_z &= \frac{\left(\frac{4\pi\gamma N}{j\omega}\right) (\langle \delta M_z^2 \rangle - \langle \delta M^2 \rangle)}{1 + \left(\frac{4\pi\gamma N}{j\omega}\right)^2 (M^2 + \langle \delta M_z^2 \rangle)} \langle h_z \rangle
\end{aligned} \tag{A18}$$

Since we are concerned only with the region $\omega_M/\omega < 1$, all terms of the form $(4\pi\gamma N/\omega)^2 (\langle \delta M^2 \rangle$ or $\langle \delta M_x^2 \rangle$ or $\langle \delta M_z^2 \rangle)$ will be much less than 1.0. We thus drop all but the most significant terms in (A18) and make use of Eqs. (A4) and (A5) leaving

$$\langle \delta \bar{M} \times \delta \bar{h} \rangle_x = \frac{\left(\frac{4\pi\gamma N}{j\omega}\right) (\langle \delta M_x^2 \rangle - \langle \delta M^2 \rangle)}{1 + \left(\frac{4\pi\gamma N}{j\omega}\right)^2 (\langle \delta M_x^2 \rangle + M^2)} \langle h_x \rangle \tag{A19a}$$

$$\langle \delta \vec{M} \times \delta \vec{H} \rangle_y = \frac{\left(\frac{4\pi\gamma N}{j\omega}\right)^2 M \langle \delta M_z^2 \rangle}{1 + \left(\frac{4\pi\gamma N}{j\omega}\right)^2 (\langle \delta M_x^2 \rangle + M^2)} \langle h_x \rangle \quad , \quad (A19b)$$

$$\langle \delta \vec{M} \times \delta \vec{H} \rangle_z = \frac{\left(\frac{4\pi\gamma N}{j\omega}\right) (\langle \delta M_z^2 \rangle - \langle \delta M^2 \rangle)}{1 + \left(\frac{4\pi\gamma N}{j\omega}\right)^2 (\langle \delta M_z^2 \rangle + M^2)} \langle h_z \rangle \quad . \quad (A19c)$$

If we now substitute Eqs. (A19) into Eq. (22) neglecting the term in $\langle \vec{H} \rangle \times \langle \vec{m} \rangle$ we obtain an approximation for $\langle \vec{m} \rangle$. If we then iterate and use this approximation in the $\langle \vec{H} \rangle \times \langle \vec{m} \rangle$ term and note the definition of permeability tensor, Eq. (7), we obtain the results given in Eqs. (25).

MICROWAVE BEHAVIOR OF PARTIALLY MAGNETIZED FERRITES *

by

Ernst Schlömann

Raytheon Research Division

Waltham, Massachusetts 02154

ABSTRACT

The high frequency permeability of partially magnetized ferrites is calculated for some simple domain configurations, comprising only "up"- and "down"-domains. The method used is based upon the magnetostatic approximation and neglects exchange effects, but is otherwise substantially rigorous. The components of the effective permeability tensor (ratio of average induction to average magnetic field) in general depends upon details of the domain configuration in addition to the net dc magnetization. When the dc magnetization is cycled between the two states of complete magnetization the high frequency permeability, considered as a function of the dc magnetization, in general shows hysteresis. Detailed calculations of the high frequency permeability have been carried out for the case in which the domain configuration is cylindrically symmetric, i. e., invariant under rotation around the direction of magnetization. For any such domain configuration the two relevant components μ_{eff} and κ_{eff} of the effective permeability tensor obey the relation $\mu_{\text{eff}}^2 - \kappa_{\text{eff}}^2 = \text{const}$, regardless of the number of domains and their relative size. This general theorem allows a simple derivation of the (isotropic) permeability in the completely demagnetized state, giving

$$\mu_{\text{eff}} = \frac{2}{3} \left\{ \left[\left(\frac{\omega}{\gamma} \right)^2 - (H_a + 4\pi M_0)^2 \right] / \left[\left(\frac{\omega}{\gamma} \right)^2 - H_a^2 \right] \right\}^{\frac{1}{2}} + \frac{1}{3}$$

where ω is the frequency, H_a the anisotropy field and M_0 the saturation magnetization.

*This research was supported in part by the Advanced Research Projects Agency of the Department of Defense and was monitored by Rome Air Development Center under Contract No. F30602-69-C-0026.

1. INTRODUCTION

In many of the applications of ferrites in microwave devices such as phaseshifters, switches and rotators the magnetic material is only partially magnetized. This mode of operation has the advantage that the microwave properties of the material can be changed significantly by the application of a rather modest magnetic field.

Because of these practical applications the microwave behavior of partially magnetized ferrites has been the subject of considerable research from the early days of the ferrite microwave technology^{1,2} until very recently.³⁻⁶ It has been found that the off-diagonal components of the susceptibility tensor are substantially proportional to the net magnetization, and that the diagonal components are negative and increase in magnitude with increasing saturation magnetization and decreasing frequency. It has also been known for a long time that the partially magnetized state is characterized by very high losses, when the frequency ω is less than, or of the order of, $\omega_M = \gamma 4\pi M_0$ (γ = gyromagnetic ratio, M_0 = saturation magnetization).

The first successful theory of the microwave behavior of partially magnetized ferrites is due to Rado.^{7,8} By suitably averaging the magnetic equation of motion and using certain simplifying assumptions concerning the correlation of magnetization and magnetic field, he deduced that the off-diagonal component of the susceptibility tensor should be given by $\gamma M/\omega$ where M is the net magnetization. This result is in quite good agreement with the experimental observations. According to Rado's theory the diagonal components of the susceptibility tensor would be expected to vanish (for zero dc magnetic field in the limit of zero loss). Similar results have also been derived by Soohoo⁹ and by Allen.¹⁰ A more refined theory, based upon a similar approach but taking the correlation of local magnetic field and local magnetization more carefully into account has recently been proposed by Sandy.¹¹ This theory yields finite diagonal components and agrees quite well with the experimental data, provided that a certain parameter which occurs in the theory (an effective rf demagnetizing factor) is properly chosen.

A very important suggestion concerning the microwave behavior of partially magnetized ferrites has been made by Polder and Smit.¹² They pointed out that in a sample containing oppositely magnetized domains the resonant frequencies of the normal modes of vibration extend upwards to the vicinity of $\gamma 4\pi M_0$. The "low field loss" generally observed in ferrites when the frequency is sufficiently low can be attributed to these Polder-Smit resonances.

Various attempts have been made to develop a quantitative theory of the microwave behavior of partially magnetized ferrites on the basis of the Polder-Smit suggestion.^{3, 4, 11, 13} These calculations are based upon some ad hoc assumptions (for instance, concerning the distribution of resonant frequencies) and are, therefore, of limited use, even though good agreement with the experimental data has been achieved in some cases.

In the present paper a new theory of the microwave behavior of partially magnetized ferrites is developed. This theory is in a certain sense complementary to those previously proposed, since it avoids many of the shortcomings of the previous theories but also has some shortcomings of its own. The microwave behavior (at low power levels) can generally be characterized by an "effective" susceptibility tensor, which relates the spatial average of the rf magnetization to the spatial average of the rf magnetic field. The aim of the theory described in the present paper is to calculate this effective susceptibility. From the magnetic equations of motion one can easily determine the "local" or "microscopic" susceptibility at any point inside the sample, if the direction of the local saturation magnetization at this point is known. The microscopic susceptibility relates the local rf magnetization to the local rf magnetic field. In order to calculate the effective susceptibility it is necessary to determine the local rf magnetic field first. In some of the previous theories this problem is circumvented by postulating a relationship between the local magnetization and the local magnetic field (an effective rf demagnetizing factor). Such a procedure can not be rigorous, because the rf magnetic field at any point

inside the material is actually not determined by the rf magnetization at that point, but rather by the distribution of rf magnetization throughout the sample. In the present theory the calculation of the local rf magnetic field is considered to be the central issue. Once this problem is solved the effective susceptibility can easily be obtained.

Because of the complexity of the problem at hand the calculation described above can only be carried out for some highly idealized domain configurations. In the present paper we confine attention to the case in which the sample contains only two types of domains, which are aligned either parallel ("up-domains") or antiparallel ("down-domains") to some reference axis (which is taken as the z-axis of the coordinate system). It is shown in Section 2 that for this case the problem of finding the local rf magnetic field reduces to solving a simple differential equation, subject to certain (not so simple) boundary conditions at the domain boundaries. A complete solution of the problem is constructed in Section 3 for the case in which the sample is a circular cylinder and contains a cylindrically symmetric domain structure. It is shown that for any domain configuration of this type the components of the effective permeability are related by a general theorem (Section 3a). Explicit results concerning the variation of the effective susceptibility with the net dc magnetization are derived for two simple examples; the case of three domains of arbitrary volume (Section 3b), and the case in which all domains of the same type have equal volume (Section 3c). The results are discussed and critically reviewed in Section 4.

2. GENERAL FORMULATION OF THE THEORY

As previously mentioned we assume that all domains are oriented either parallel or antiparallel to the z -axis. This represents a stable domain configuration provided that the domains are cylinders whose axes are aligned with the z -axis. The cylinders can have arbitrary cross-sections in the x - y plane as shown in Fig. 1. The domains in which the dc magnetization is parallel to the positive z -axis (up-domains) are denoted by the subscript u , those in which it is antiparallel to the positive z -axis (down-domains) by the subscript d .

The local permeability is the same throughout each type of domain, but differs from one type of domain to the other. We characterize the x and y components of the local permeability tensors for the two types of domains by

$$\vec{\mu}_u = \begin{pmatrix} \mu_u & -i\kappa_u \\ i\kappa_u & \mu_u \end{pmatrix} \quad \vec{\mu}_d = \begin{pmatrix} \mu_d & i\kappa_d \\ -i\kappa_d & \mu_d \end{pmatrix} \quad (1)$$

The tensor components μ and κ can easily be calculated from the magnetic equations of motion. If loss is neglected, one finds

$$\mu_{u,d} = 1 + \frac{H_{u,d} 4\pi M_0}{H_{u,d}^2 - (\omega/\gamma)^2}$$

$$\kappa_{u,d} = - \frac{4\pi M_0 \omega/\gamma}{H_{u,d}^2 - (\omega/\gamma)^2}, \quad (2)$$

where $H_{u,d}$ is the effective dc magnetic field strength in the direction of the (local) dc magnetization. If the material has uniaxial crystalline anisotropy the effective dc magnetic field arising from this source would be the same

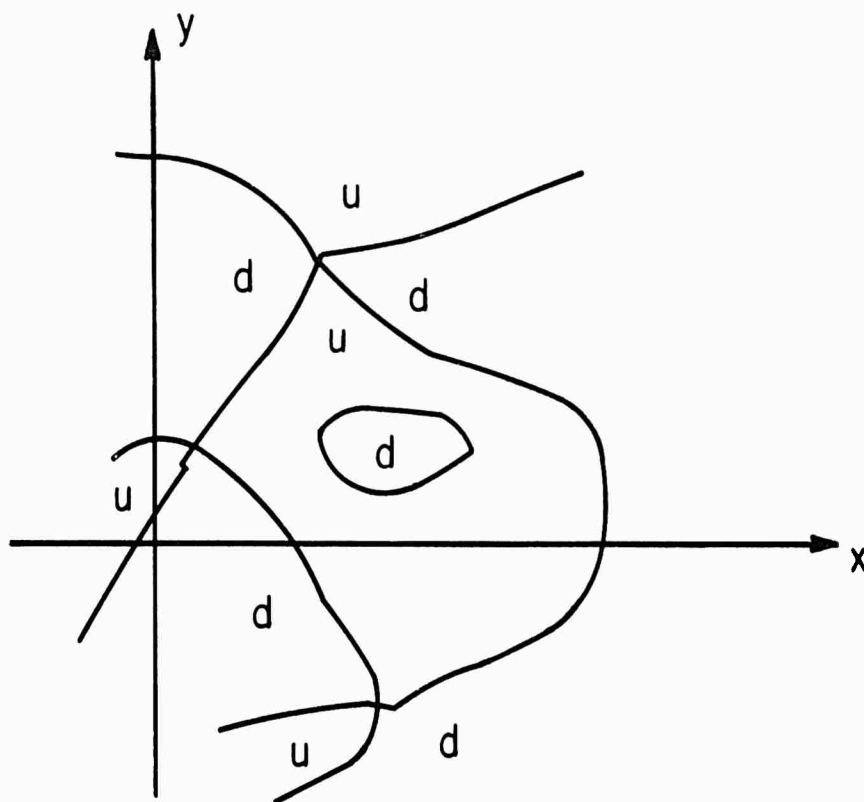


Fig. 1 Domain configuration as assumed in Sec. 2. The domains are cylinders with arbitrary cross section whose axes are aligned with the z -axis.

in both types of domains. An externally applied dc magnetic field, if it is not compensated by demagnetizing fields, would add to the effective dc field in one type of domain and subtract from that in the other. Actually the applied field is almost entirely compensated by demagnetizing fields. By way of approximation it is, therefore, permissible to set $\mu_u = \mu_d$, $\kappa_u = \kappa_d$. In the following we adopt this approximation for the sake of simplicity. Furthermore, the anisotropy field is usually much smaller than ω/γ . Under these conditions Eq. (2) can be approximated by

$$\mu = 1 \quad , \quad \kappa = \omega_M/\omega \quad (3)$$

where $\omega_M = \gamma 4\pi M_0$.

The effect of dissipation upon the local permeability can be taken into account by adding a phenomenon logical damping term to the equations of motion. μ and κ are then in general complex. In the limit of zero effective magnetic field the tensor components are now

$$\mu = 1 - i\delta \quad , \quad \kappa = \omega_M/\omega \quad (4)$$

The off-diagonal tensor component κ is real in this limit. δ is related to the "effective" linewidth ΔH_{eff} ¹⁴ that characterizes the losses of the saturated material in the region of very small dc fields by

$$\delta \approx \gamma^2 2\pi M_0 \Delta H_{\text{eff}}/\omega^2 \quad (5)$$

If the profile of the resonance line is Lorentzian the effective linewidth that occurs in Eqs. (4) and (5) equals the width ΔH of the resonance peak. In many polycrystals, however, ΔH_{eff} is much smaller than ΔH .

Consider now the rf magnetic field $\mathbf{h}(\mathbf{r})$ associated with some arbitrary distribution of the rf magnetization $\mathbf{m}(\mathbf{r})$. We calculate this field subject to the quasistatic approximation. Thus $\mathbf{h}(\mathbf{r})$ can be represented as the gradient of a potential $\Psi(\mathbf{r})$

$$\underline{h} = \nabla \Psi \quad . \quad (6)$$

Since the divergence of $\underline{b} = \frac{1}{\mu} \cdot \underline{h}$ vanishes the potential Ψ satisfies the differential equation

$$\left[\mu \left(\frac{\partial^2}{\partial x^2} + \frac{\partial^2}{\partial y^2} \right) + \frac{\partial^2}{\partial z^2} \right] \Psi = 0 \quad (7)$$

which is well-known from the theory of magnetostatic modes.^{15, 16} It should be noticed that the same equation (7) applies in both types of domains.

In the present context we need to consider only such field distributions that are independent of z . In this case the differential equation that determines Ψ reduces to the two-dimensional Laplace equation

$$\left(\frac{\partial^2}{\partial x^2} + \frac{\partial^2}{\partial y^2} \right) \Psi = 0 \quad . \quad (8)$$

The boundary conditions to which the potential is subject arise from the requirement that the tangential component of the magnetic field \underline{h} and the normal component of the magnetic induction \underline{b} must be continuous. Let $\partial\Psi/\partial s$ denote the tangential derivative and $\partial\Psi/\partial n$ the normal derivative of the potential taken at the domain boundary. The potential Ψ_u and Ψ_d (applicable inside the up- and down-domains respectively) then has to satisfy the conditions

$$\frac{\partial \Psi_u}{\partial s} = \frac{\partial \Psi_d}{\partial s}$$

$$\mu \left(\frac{\partial \Psi_u}{\partial n} - \frac{\partial \Psi_d}{\partial n} \right) = i\kappa \left(\frac{\partial \Psi_u}{\partial s} + \frac{\partial \Psi_d}{\partial s} \right) \quad . \quad (9)$$

Here it is assumed that n, s, z constitutes a right-handed coordinate system (as does x, y, z).

In the following it will be assumed that the sample is surrounded by air. In the exterior of the sample the potential Ψ , therefore, also satisfies the Laplace equation (8). At the sample boundary the tangential component of \underline{h} and the normal components of \underline{b} are continuous.

Assume now that the differential equation for the potential has been solved subject to all the boundary conditions at the domain boundaries and the sample surface. How is this solution related to the microwave behavior that is directly observable?

The magnetic response of a small sample of ellipsoidal shape can be characterized by the "internal" or the "external" effective susceptibility. The former relates the average rf magnetization to the average rf magnetic field inside the sample, the latter relates it to the rf magnetic field existing outside the sample. For experiments with small samples the external susceptibility is more closely related to the directly observed physical quantities (e. g., change of frequency and $1/Q$ of a resonant cavity). The internal susceptibility, on the other hand, is a more fundamental quantity, because it is not dependent upon the shape of the sample. We shall, therefore, state our results in terms of the internal effective susceptibility. It is well known that the two types of susceptibilities are related by

$$\chi_{\text{ex}} = (1 + 4\pi \chi_{\text{in}} N_t)^{-1} \chi_{\text{in}} \quad (10)$$

where N_t is the transverse demagnetizing factor. All susceptibilities and permeabilities mentioned in the remainder of the paper are "internal". The subscript "in" will henceforth be omitted.

The microwave behavior of partially magnetized ferrites can most economically be characterized by the "circular" susceptibility, i. e., the response to a rotating rf magnetic field. If the domain structure does not distinguish any direction in the x-y plane on a macroscopic scale the susceptibility tensor must be diagonal with respect to such a rotating magnetic

field. We calculate primarily the effective circular permeability $\mu_{+ \text{eff}}(\omega)$ for the positive sense of rotation. The corresponding permeability for the negative sense of rotation is then obtained by inverting the sign of the frequency and taking the complex conjugate

$$\mu_{- \text{eff}}(\omega) = \mu_{+ \text{eff}}^*(-\omega) \quad (11)$$

The effective permeability tensor has the same structure as the local permeability tensor [given by Eq. (1)] except that the components μ_{eff} and κ_{eff} are now defined by

$$\mu_{\pm \text{eff}} = \mu_{\text{eff}} \mp \kappa_{\text{eff}} \quad (12)$$

In the next section the calculation of the effective permeability is explicitly carried out for a simple domain structure.

3. APPLICATION TO SAMPLES WITH CYLINDRICAL DOMAIN STRUCTURE

3a. General Discussion

Consider now a sample in the shape of a circular cylinder, with a cylindrically symmetric domain structure such as shown in Fig. 2. We assume (arbitrarily) that the domain at the core of the cylinder is a down-domain. The significance of this assumption is further discussed later in this section. The outer radii of the domains are denoted by r_n ($n = 1, 2, \dots, N$).

The fundamental solutions of Laplace's equation in cylindrical coordinates are

$$\Psi = r^m e^{-im\phi}, \quad r^{-m} e^{-im\phi} \quad (13)$$

where m is a positive integer. Consider the first of these solutions for $m = 1$, i. e., $\Psi = r e^{-i\phi} = x - iy$. Since the time dependence is assumed to be $\exp(i\omega t)$ it follows that the magnetic field associated with this potential is

$$\begin{aligned} h_x &= \operatorname{Re} e^{i\omega t} = \cos \omega t \\ h_y &= \operatorname{Re} (-i e^{i\omega t}) = \sin \omega t \end{aligned} \quad (14)$$

Thus for $m = 1$ the first potential in Eq. (13) describes a rotating, uniform magnetic field. The sense of rotation depends upon the sign of ω , being positive for positive ω . In addition to the solutions given by Eq. (13) the Laplace equation also admits solution of the form $r^m e^{im\phi}$ and $r^{-m} e^{im\phi}$. The fields associated with these potentials are identical with those of the potentials given by Eq. (13) provided that the sign of ω is reversed. Thus these additional solutions need not be considered separately in the calculation if ω is allowed negative as well as positive values.

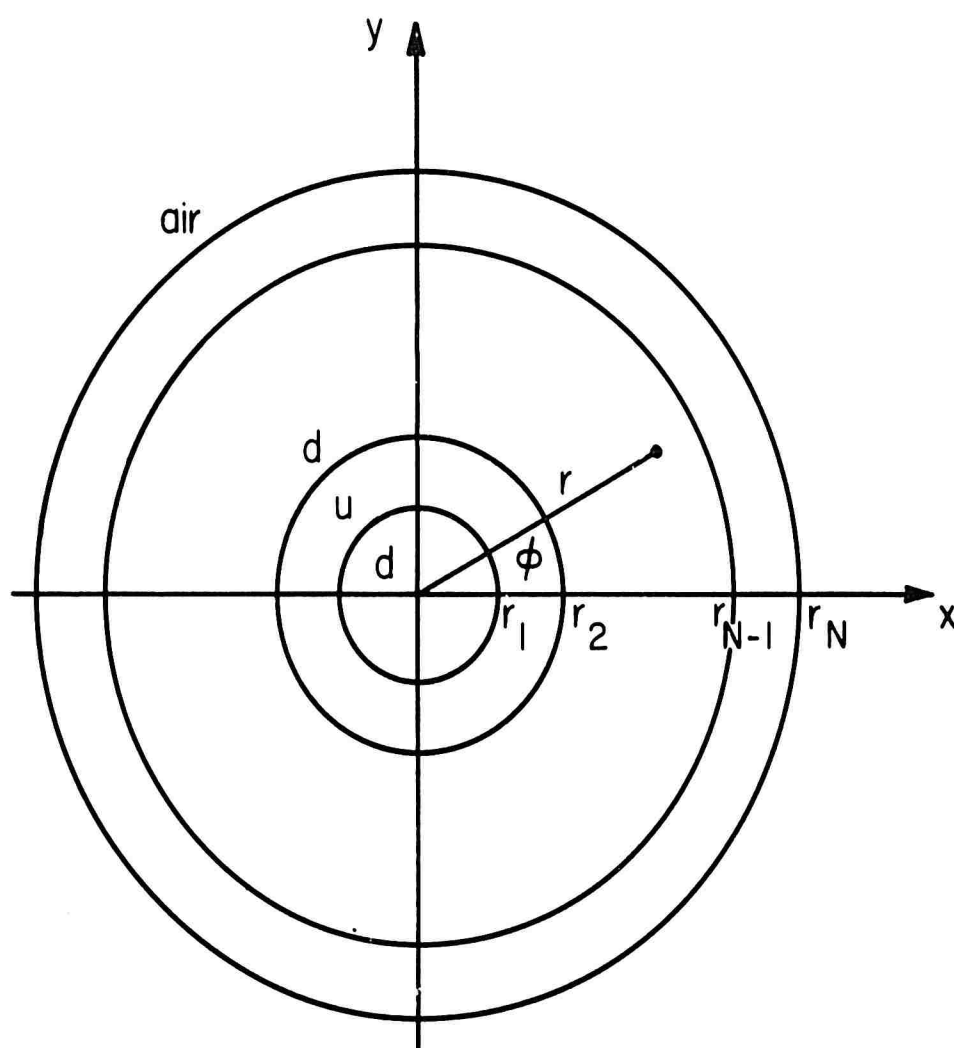


Fig. 2 Cylindrically symmetric domain configuration as assumed in Sec. 3.

In general the potential inside each domain as well as in the exterior of the sample can be expanded in terms of the fundamental solutions given by Eq. (13). In the present context we can confine attention to those potentials that describe an rf magnetic field which reduces to a homogeneous rotating field at points far away from the sample. For $r \rightarrow \infty$ the potential must be of the form

$$\Psi(r \rightarrow \infty) = h_0 r e^{-i\phi} \quad (15)$$

where h_0 is the amplitude of the rotating magnetic field. Because of the orthogonality of the exponential functions for different m , the expansion of the potential inside the sample then also contains only the terms corresponding to $m = 1$. Thus the potential for the n^{th} domain is

$$\psi_n = (A_n r + B_n r^{-1}) e^{-i\phi} \quad (16)$$

where A_n and B_n are arbitrary coefficients, to be determined by the boundary condition. For the core-domain ($n = 1$)

$$B_1 = 0 \quad (17)$$

to avoid a singularity at $r = 0$. For the region outside the sample ($n = N + 1$)

$$A_{N+1} = h_0 \quad (18)$$

to conform with Eq. (15).

The radial and circumferential components of \underline{h} and \underline{b} inside the n^{th} domain are according to Eqs. (16), (6) and (1)

$$h_{rn} = (A_n - B_n r^{-2}) e^{-i\phi}$$

$$h_{\phi n} = -i (A_n + B_n r^{-2}) e^{-i\phi}$$

$$b_{rn} = [(\mu \mp \kappa) A_n - (\mu \pm \kappa) B_n r^{-2}] e^{-i\phi}$$

$$b_n = -i [(\mu \mp \kappa) A_n + (\mu \pm \kappa) B_n r^{-2}] e^{-i\phi} \quad (19)$$

Here the upper signs refer to up domains, the lower sign to down domains. Thus the boundary conditions at r_1 are (since $B_1 = 0$)

$$A_1 = A_2 + B_2 r_1^{-2}$$

$$(\mu + \kappa) A_1 = (\mu - \kappa) A_2 - (\mu + \kappa) B_2 r_1^{-2} \quad (20)$$

Similarly at r_n ($n = 2, 3, \dots, N-1$)

$$A_n + B_n r_n^{-2} = A_{n+1} + B_{n+1} r_n^{-2}$$

$$(\mu \mp \kappa) A_n - (\mu \pm \kappa) B_n r_n^{-2} = (\mu \pm \kappa) A_{n+1} - (\mu \mp \kappa) B_{n+1} r_n^{-2} \quad (21)$$

where the upper sign again refers to up domains (even n), the lower to down domains (odd n). At the sample boundary (r_N) according to Eq. (18)

$$A_N + B_N r_N^{-2} = h_0 + B_{N+1} r_N^{-2}$$

$$(\mu \mp \kappa) A_N - (\mu \pm \kappa) B_N r_N^{-2} = h_0 - B_{N+1} r_N^{-2} \quad (22)$$

Equations (20-22) constitute an inhomogeneous set of $2N$ linear equations for the $2N$ arbitrary coefficients A_n and B_n . Each of these coefficients is, therefore, uniquely determined. Not surprisingly, each is proportional to h_0 .

Consider now the spatial average of the rf magnetic field and the rf magnetic induction. The x- and y- components of the magnetic field inside the n^{th} domain are according to Fig. 2 and Eq. (19)

$$\begin{aligned} h_{xn} &= h_{rn} \cos \phi - h_{\phi n} \sin \phi = A_n - B_n r^{-2} e^{-2i\phi} \\ h_{yn} &= h_{rn} \sin \phi + h_{\phi n} \cos \phi = -i [A_n + B_n r^{-2} e^{-2i\phi}] \end{aligned} \quad (23)$$

The contribution of the B-coefficients vanishes when averaged over ϕ . It can be shown by substantially the same reasoning that this is also true for the rf magnetic induction. Thus only the A-coefficients contribute to the average magnetic field and to the average magnetic induction.

In order to obtain the effective circular permeability we have to take the ratio of the spacial averages of the magnetic induction and the magnetic field. Thus

$$\mu_{+ \text{ eff}} = \frac{(\mu + \kappa) r_1^2 A_1 + (\mu - \kappa) (r_2^2 - r_1^2) A_2 + (\mu + \kappa) (r_3^2 - r_2^2) A_3 + \dots}{r_1^2 A_1 + (r_2^2 - r_1^2) A_2 + (r_3^2 - r_2^2) A_3 + \dots} \quad (24)$$

For further progress the coefficients A_n must be determined. For convenience we define a "vector"

$$\underline{A}_n = \begin{pmatrix} A_n \\ B_n \end{pmatrix} \quad (25)$$

Equation (21) is then equivalent to

$$\underline{A}_{n+1} = \underline{M}_n \underline{A}_n \quad (26)$$

where the matrix \underline{M}_n is given by

$$M_n = \begin{pmatrix} 1 \mp \sigma & \mp \sigma r_n^{-2} \\ \pm \sigma r_n^2 & 1 \pm \sigma \end{pmatrix} \quad (27)$$

(upper sign for even n , lower for odd n as before). Here

$$\sigma = \kappa/\mu \quad . \quad (28)$$

Equation (26) holds also for $n = 1$ except that in this case $B_1 = 0$ [compare Eq. (20)]. Using Eq. (26) all coefficients A_n ($n = 2, 3, \dots$) can readily be expressed in terms of A_1 .

It is apparent from the preceding results [in particular Eq. (24)] that the effective permeability in general depends upon details of the domain configuration (such as the number of domains and their size) as well as upon gross features (such as the net dc magnetization). For any reasonably complex domain structure the theory, therefore, yields a result which depends upon a vast number of adjustable parameters. This may facilitate obtaining a good fit to experimental data, but the significance of such a fit is doubtful unless it can be shown that the domain structure actually present is similar to that assumed in the calculation.

It is fortunate, therefore, that certain results of the theory are not dependent upon the details of the domain configuration. It is shown in Appendix 1 that for any cylindrically symmetric, but otherwise arbitrary domain configuration

$$\mu_{\text{eff}}^2 - \kappa_{\text{eff}}^2 = \mu^2 - \kappa^2 \quad . \quad (29)$$

This theorem has several interesting consequences. It is known from Rado's work^{7,8} that κ_{eff} is substantially proportional to the net magnetization. (The present theory gives similar results, as further discussed in Sections 3b and 3c.) Since the right hand side of Eq. (29) is independent of the domain

configuration, it follows that μ_{eff} , considered as a function of the net magnetization goes through a minimum at that magnetization at which κ_{eff} vanishes. The minimum value of μ_{eff} is independent of the domain configuration being given [according to Eqs. (29) and (2)] by

$$\mu_{\text{eff min}} = \left[\frac{(\omega/\gamma)^2 - (H_a + 4\pi M_0)^2}{(\omega/\gamma)^2 - H_a^2} \right]^{\frac{1}{2}} \quad (30)$$

Here it has been assumed that the effective magnetic field inside the domains is the anisotropy field H_a . For a sample containing many very small domains the state of vanishing κ_{eff} is very close to that of vanishing net magnetization. Thus the effective permeability given by Eq. (30) can be identified with that applicable in the completely demagnetized state. It should be noticed that it is real for $\omega/\gamma > H_a + 4\pi M_0$ but imaginary for $H_a < \frac{\omega}{\gamma} < H_a + 4\pi M_0$. With suitable corrections to allow for the random orientation of the domains and for the finite linewidth of the material Eq. (30) has been found to agree quite well with the observed behavior of the real and imaginary parts of μ_{eff} in the demagnetized state.

3b. Application to Samples Containing Only Three Domains

In this section and the one following the general results derived in the preceding section are explicitly evaluated for two special cases. The results given in Section 3b apply to a sample containing only three domains (of arbitrary volume), those given in Section 3c to a sample containing an even number N ($N = 2, 4, 6, 10, 20, 40, 80$) of domains provided that domains of the same type have equal volume. In both of these cases the results depend upon a single "adjustable" parameter as well as upon the net magnetization. In the three-domain case the adjustable parameter is the volume ratio of the two down-domain; in the many-domain case this parameter is the total number (N) of domains. According to Eqs. (25) and (26)

$$A_2 = (1 + \sigma) A_1$$

$$A_3 = [1 - \sigma^2 + \sigma^2 (r_1/r_2)^2] A_1 \quad (31)$$

The relative dc magnetization (i. e., the volume difference of up-domains and down-domains divided by the total volume) is

$$\zeta = (2r_2^2 - 2r_1^2 - r_3^2)/r_3^2 \quad (32)$$

and the volume ratio of the two down-domains

$$\rho = (r_3^2 - r_2^2)/r_1^2 \quad (33)$$

After trivial calculations one obtains from Eqs. (24) and (31-33)

$$\frac{\mu_{+ \text{ eff}}}{\mu} = 1 - \sigma \frac{\zeta + \sigma \frac{1+\zeta}{2} + \sigma^2 \frac{\rho(1-\zeta^2)}{2[2+\rho(1+\zeta)]}}{1 + \sigma \frac{1+\zeta}{2} - \sigma^2 \frac{\rho(1-\zeta^2)}{2[2+\rho(1+\zeta)]}} \quad (34)$$

Consider now the real parts of the components of the internal effective susceptibility tensor. As long as $\omega_M/\omega \lesssim 0.9$ the losses have only a very small influence on these components, and are therefore neglected in this discussion. According to Eqs. (34), (11), (12) and (3) taking σ as real

$$\frac{\mu'_{\text{eff}}}{\mu} = 1 - \frac{1}{2} \sigma^2 (1 - \zeta^2) \left[1 - \sigma^2 \rho \frac{1 + \zeta}{2 + \rho(1 + \zeta)} \right] / W$$

$$\frac{\kappa'_{\text{eff}}}{\mu} = \sigma \left\{ \zeta + \frac{\sigma^2}{4} \left[\frac{2\rho(1-\zeta^2)(1-\zeta)}{2+\rho(1+\zeta)} - (1+\zeta)^2 \right] - \left[\frac{\sigma^2 \rho(1-\zeta^2)}{2[2+\rho(1+\zeta)]} \right]^2 \right\} / W \quad (35)$$

where

$$W = 1 - \sigma^2 \left[\frac{\rho(1 - \zeta^2)}{2 + \rho(1 + \zeta)} + \frac{1}{4} (1 + \zeta)^2 \right] + \left[\frac{\sigma^2 \rho (1 - \zeta^2)}{2(2 + \rho(1 + \zeta))} \right]^2 \quad (36)$$

If $H_a \ll \omega/\gamma$ we may approximate σ by ω_M/ω . It may be seen that for $\sigma \ll 1$ the leading term in κ'_{eff} is $\sigma\zeta = \gamma 4\pi M/\omega$ in agreement with Rado's result. It should be noticed, however, that κ'_{eff} as given by Eq. (35) does not necessarily vanish for $\zeta = 0$.

In Figs. 3 and 4 the tensor components μ'_{eff} and κ'_{eff} are plotted versus relative magnetization ζ for $\omega_M/\omega = 0.9$ and different fixed values of the parameter ρ assuming $H_a = 0$. For comparison the result of Rado's theory is also shown in Fig. 4 as a broken line. It may be seen that for $\rho = 4$ the μ'_{eff} versus ζ curve is approximately symmetric, the κ'_{eff} versus ζ curve approximately antisymmetric in ζ . In this connection it is important to remember that the calculation as presented is based upon the assumption that the core-domain is magnetized "down". The curves applicable for the case in which the core-domain is magnetized "up" can be obtained by reflecting the μ -curves around the vertical axis and the κ -curves around origin. When the static magnetization is cycled between the completely magnetized states the core-domain will most likely reverse its direction at each half cycle. The effective permeabilities will, therefore, exhibit a hysteresis when plotted as a function of the static magnetization. Such hysteresis effects are indeed observed experimentally.⁵

The effect of a finite anisotropy field upon the curves shown in Figs. 3 and 4 can easily be taken into account. In Eqs. (35) and (36) the anisotropy field enters only through σ and μ . Since the curves are valid for a given σ , they apply for any combination of $4\pi M_0$, ω , and H_a for which $\sigma = \kappa/\mu = \omega_M \omega / [\omega^2 - \gamma^2 H_a (H_a + 4\pi M_0)]$ has the appropriate value. The ordinate then represents μ'_{eff}/μ and κ'_{eff}/μ rather than μ'_{eff} and κ'_{eff} itself. The curves shown in Figs. 3 and 4 apply for instance also when $\omega_M/\omega = 0.817$, $\gamma H_a/\omega = 0.1$. The value of μ'_{eff} in the completely magnetized states (i. e., $\zeta = \pm 1$) is smaller than unity when the anisotropy field is finite.

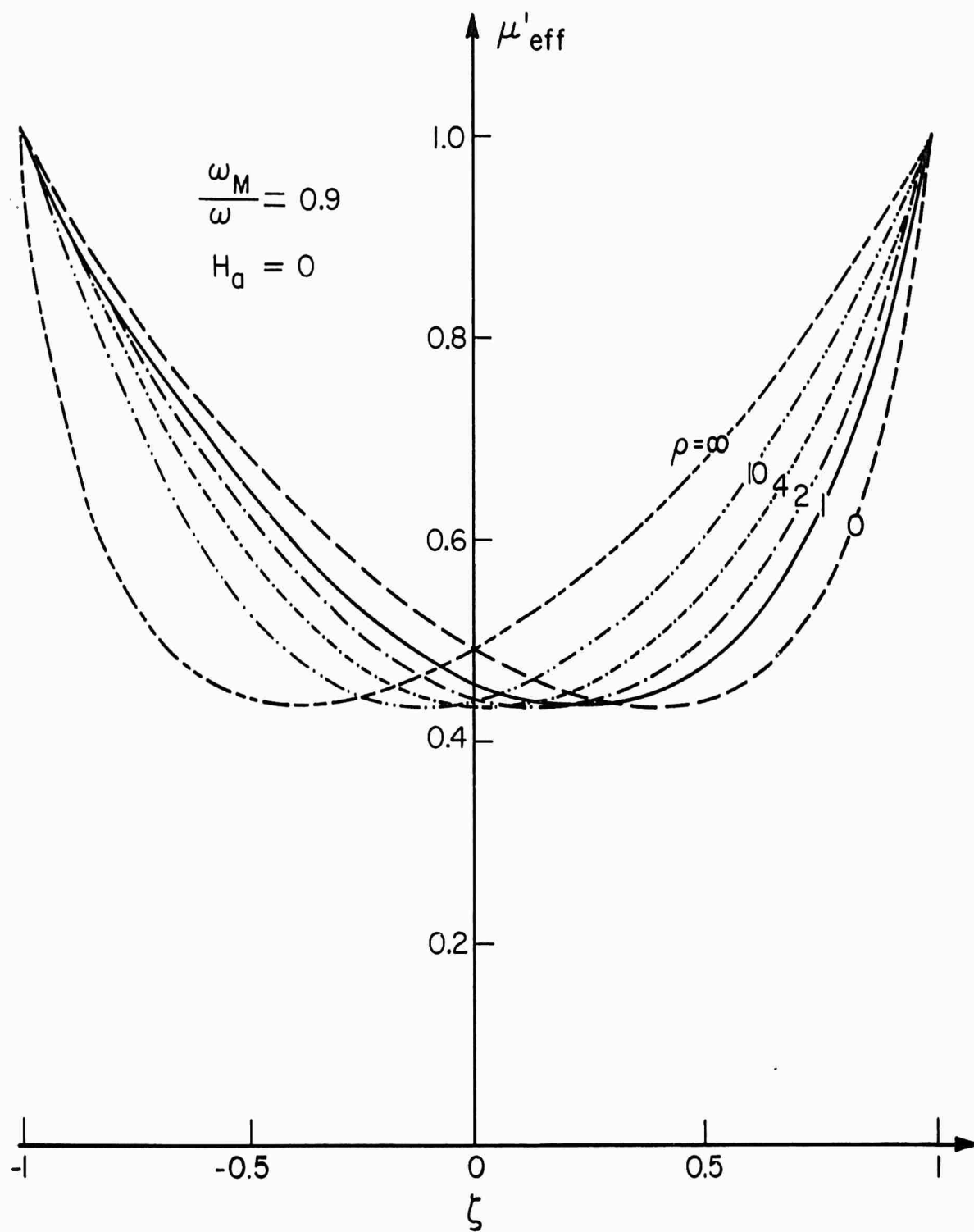


Fig. 3. Real part of the diagonal component of the effective permeability μ'_{eff} vs reduced magnetization ζ . The curves apply to a three-domain configuration for $\omega_M/\omega = 0.9$, $H_a = 0$, and several assumed values of ρ .

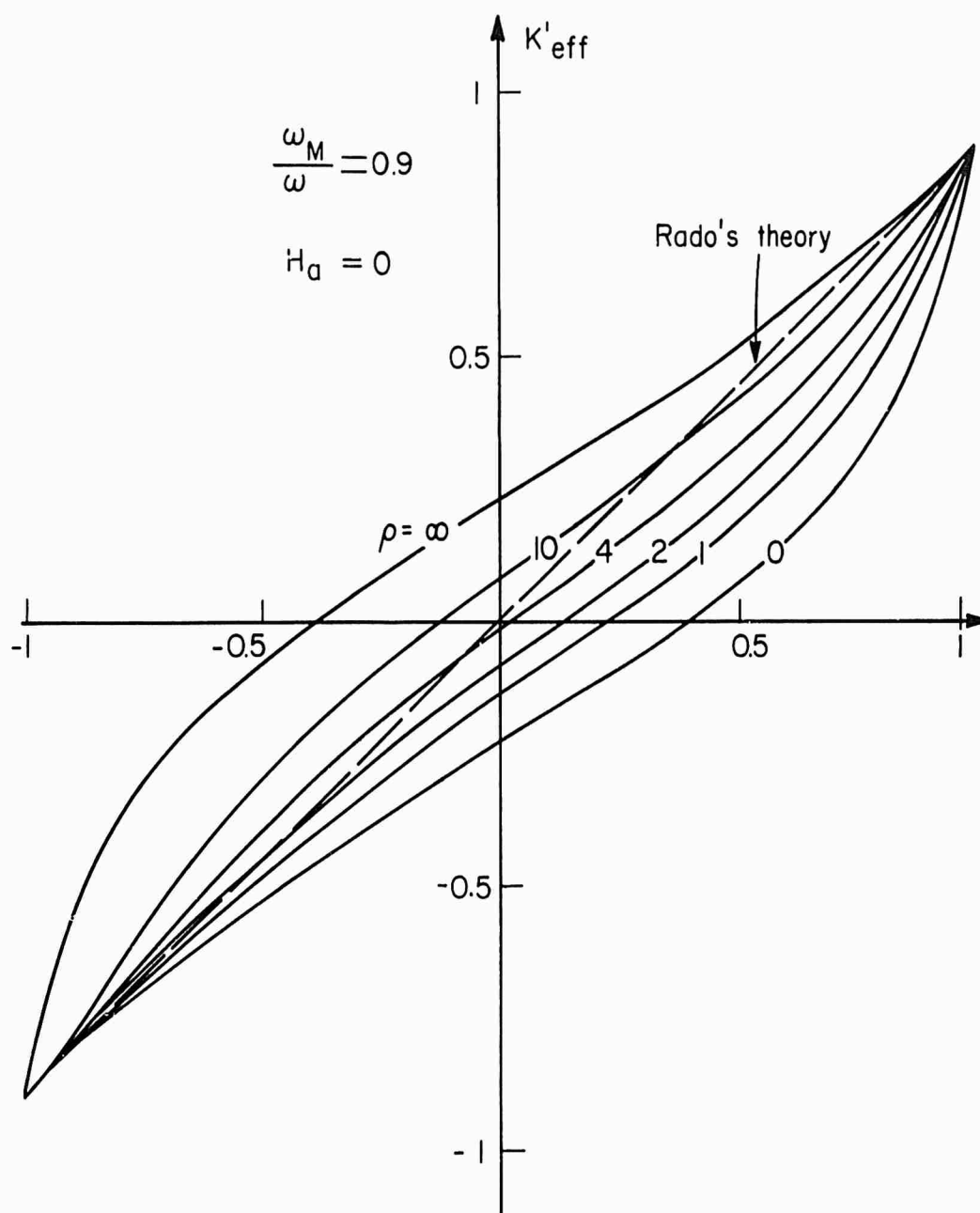


Fig. 4. Real part of the off-diagonal component of the effective permeability κ'_{eff} vs reduced magnetization ζ . The curves apply to a three-domain configuration for $\omega_M/\omega = 0.9$, $H_a = 0$, and several assumed values of ρ .

Consider now the imaginary parts of the effective circular permeabilities. For simplicity we confine attention to the case in which the anisotropy field is negligible, i. e., the microscopic permeability is given by Eq. (4). According to Eqs. (34), (11), and (4) we can generally express the imaginary parts of the effective circular permeabilities as

$$\mu_{\pm \text{ eff}}'' = \delta(1 + C_{\pm}/D_{\pm}) \quad (37)$$

where

$$C_{\pm} = \sigma_0^2 \frac{(1-\zeta^2)}{2} \left\{ 1 + \delta^2 \pm 2\sigma_0 \frac{\rho(1+\zeta)}{2+\rho(1+\zeta)} + \sigma_0^2 \frac{\rho^2(1+\zeta)}{2+\rho(1+\zeta)} \right\} \quad (38)$$

$$D_{\pm} = \left[1 - \delta^2 \pm \sigma_0 \frac{1+\zeta}{2} - \sigma_0^2 \frac{\rho}{2} \frac{1-\zeta^2}{2+\rho(1+\zeta)} \right]^2 + \delta^2 \left[2 \pm \sigma_0 \frac{1+\zeta}{2} \right]^2 \quad (39)$$

and $\sigma_0 = \omega_M/\omega$.

In most cases of interest the loss parameter δ is $\ll 1$ [compare Eq. (15)]. For $\sigma_0 < 1$ the first bracket in Eq. (39) does not vanish anywhere in the interval $-1 < \zeta < 1$. Under these conditions C_{\pm} and D_{\pm} can be replaced by their limit for $\delta \rightarrow 0$ by way of approximation.

In Fig. 5 the imaginary parts of the two circular permeabilities as calculated on this basis from Eqs. (37), (38) and (39) are shown as functions of the relative magnetization for $\omega_M/\omega = 0.9$ and various values of ρ . The tensor components μ_{eff}'' and κ_{eff}'' can be obtained from these curves in accordance with Eq. (12) by taking half the sum and half the difference of $\mu_{+ \text{ eff}}''$ and $\mu_{- \text{ eff}}''$. Again the results as shown are based upon the assumption that the core domain is magnetized down. The results for the case in which the core domain is magnetized up are obtainable by reversing the sign of ζ and simultaneously interchanging μ_{+} and μ_{-} . Comparison of Fig. 5 with Figs. 3 and 4 shows that the imaginary parts of the permeability show more hysteresis than the real parts.

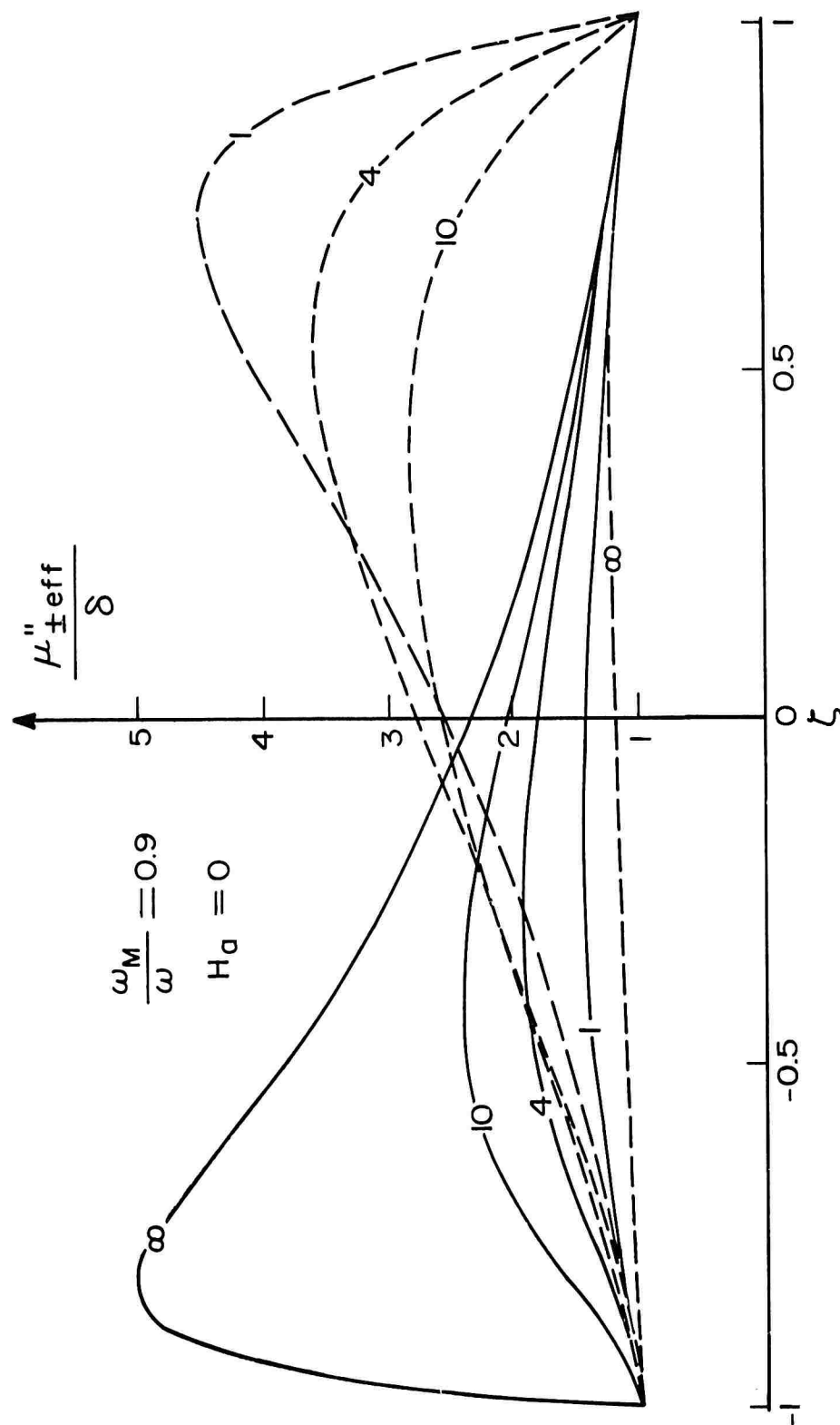


Fig. 5. Absorption coefficients for circular polarization $\mu_{\pm \text{eff}}''$ vs reduced magnetization ζ . The curves apply to a three-domain configuration for $\omega_M = 0.9$, $H_a = 0$, and several assumed values of ρ . Solid lines correspond to positive, broken lines to negative circular polarization.

It is interesting to note that the absorption coefficient for the negative sense of circular polarization shows a peak in the region of positive net magnetization ($\zeta > 0$), whereas the absorption coefficient for positive polarization shows a peak in the region of negative net magnetization ($\zeta < 0$). Thus the absorption in general peaks for the "anti-Larmor" sense of circular polarization, i. e., that sense (defined with respect to the direction of the net magnetization) which does not excite the ordinary ferromagnetic resonance of a completely magnetized material. This result is in agreement with the experimental observations of LeCraw and Spencer² and Sandy.⁵ Qualitatively the effect can be attributed to the fact that a small down-domain surrounded by a large up-domain has a high resonant frequency (approaching ω_M) and that this resonance is excited by that sense of circular polarization which couples best to the down domain (i. e., the negative sense of polarization in our terminology). This is substantially the qualitative explanation given by LeCraw and Spencer,² which is confirmed by the more rigorous theory presented in the present paper.

In Fig. 6 the absorption coefficients for the two senses of circular polarization are plotted versus ζ for $\omega_M/\omega = 0.5$. It may be seen that, compared to the case $\omega_M/\omega = 0.9$ (see Fig. 5), the absorption is now much smaller. In particular the difference between μ''_+ and μ''_- (i. e., $2k''$) is minute compared to the sum (i. e., $2\mu''$). This is again in qualitative agreement with many experimental observations.⁵

For $\sigma_0 \gtrsim 1$ it is no longer permissible to approximate D_{\pm} by its limit for $\delta \rightarrow 0$, even when $\delta \ll 1$, because the first bracket in Eq. (39) can now vanish for certain values of ζ and ρ . This is the Polder-Smit resonance mentioned in the introduction which accounts for the onset of "low field loss".

Some examples of the dependence of the absorption coefficients upon the reduced magnetization to be expected under these conditions are shown

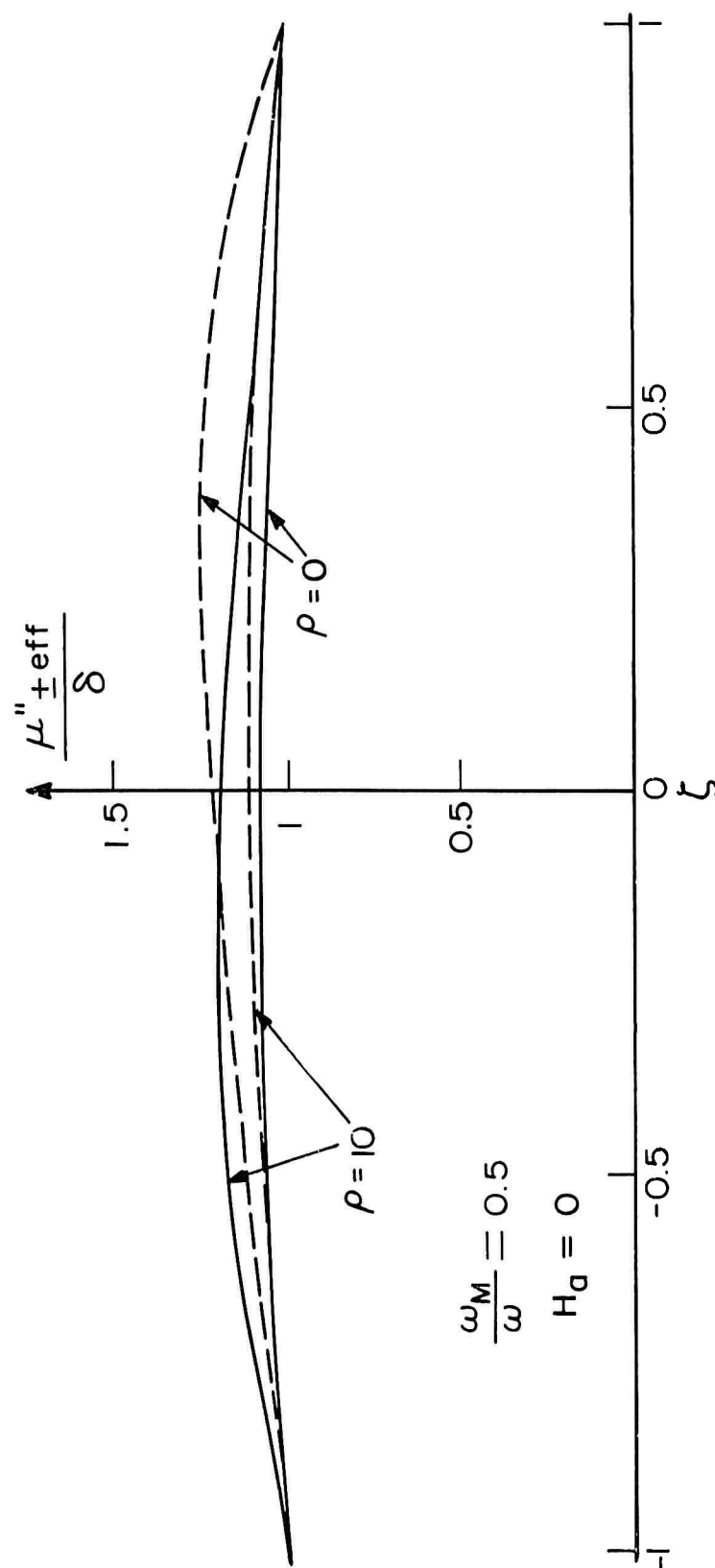


Fig. 6 Absorption coefficients for circular polarization μ''_{\pm} vs reduced magnetization ζ . The curves apply to a three-domain configuration for $\omega_M/\omega = 0.5$, $H_a = 0$, and several assumed values of ρ . Solid lines correspond to positive, broken lines to negative circular polarization.

in Figs. 7 and 8. In these examples ρ has been chosen as 4 and δ as 10^{-2} . $\mu_{\text{eff}}''/\delta$ versus ζ is shown in Fig. 7 for $\sigma_0 = 0.9, 1, 1.1$ and 1.2 . It may be seen that near $\sigma_0 = 1$ the absorption increases very rapidly with σ_0 for almost all values of ζ . The same is true, though to a lesser extent, for μ_{eff}'' as shown in Fig. 8.

3c. Application to Samples Containing an Even Number of Domains, Domains of the Same Type Having Equal Volume

Let p and q be the fractional area occupied by up and down domains, respectively. Thus

$$p + q = 1 \quad (40)$$

and the relative net magnetization is

$$\zeta = p - q \quad (41)$$

It is shown in Appendix 2 that for a cylindrically symmetric arrangement of up and down domains the components of the effective permeability tensor can be expressed as

$$\begin{aligned} \frac{\mu_{\text{eff}}}{\mu} &= 1 - \sigma^2 \frac{2 y(\sigma)}{[y(\sigma) + 1]^2 - \sigma^2} \\ \frac{\kappa_{\text{eff}}}{\mu} &= \sigma \frac{1 - \sigma^2 - y(\sigma)^2}{[y(\sigma) + 1]^2 - \sigma^2} \end{aligned} \quad (42)$$

where

$$y(\sigma) = q f_N(\sigma) / p g_N(\sigma) \quad (43)$$

and $f_N(\sigma)$ and $g_N(\sigma)$ are defined by Eq. (A13) in terms of the (1, 1) components of matrices $\underline{S}(\sigma)$ and $\underline{T}(\sigma)$ given by Eq. (A9). For $N = 2$ and 4 these matrices

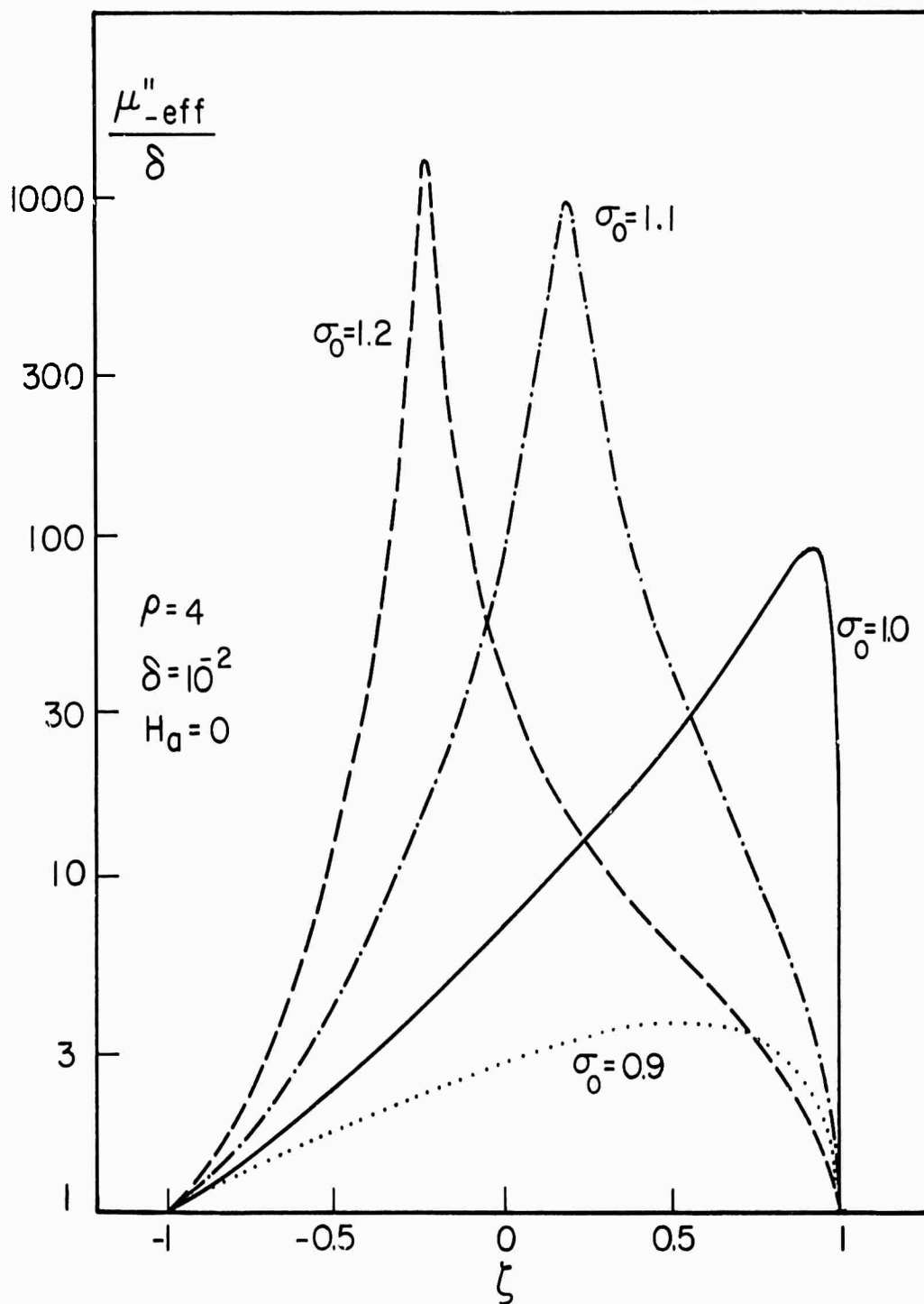


Fig. 7 Absorption coefficient for negative circular polarization μ''_{eff} vs reduced magnetization ζ . The curves apply to a three-domain configuration for $\rho = 4$, $\delta = 10^{-2}$, $\omega_M = 0.9 - 1.2$, and $H_a = 0$.

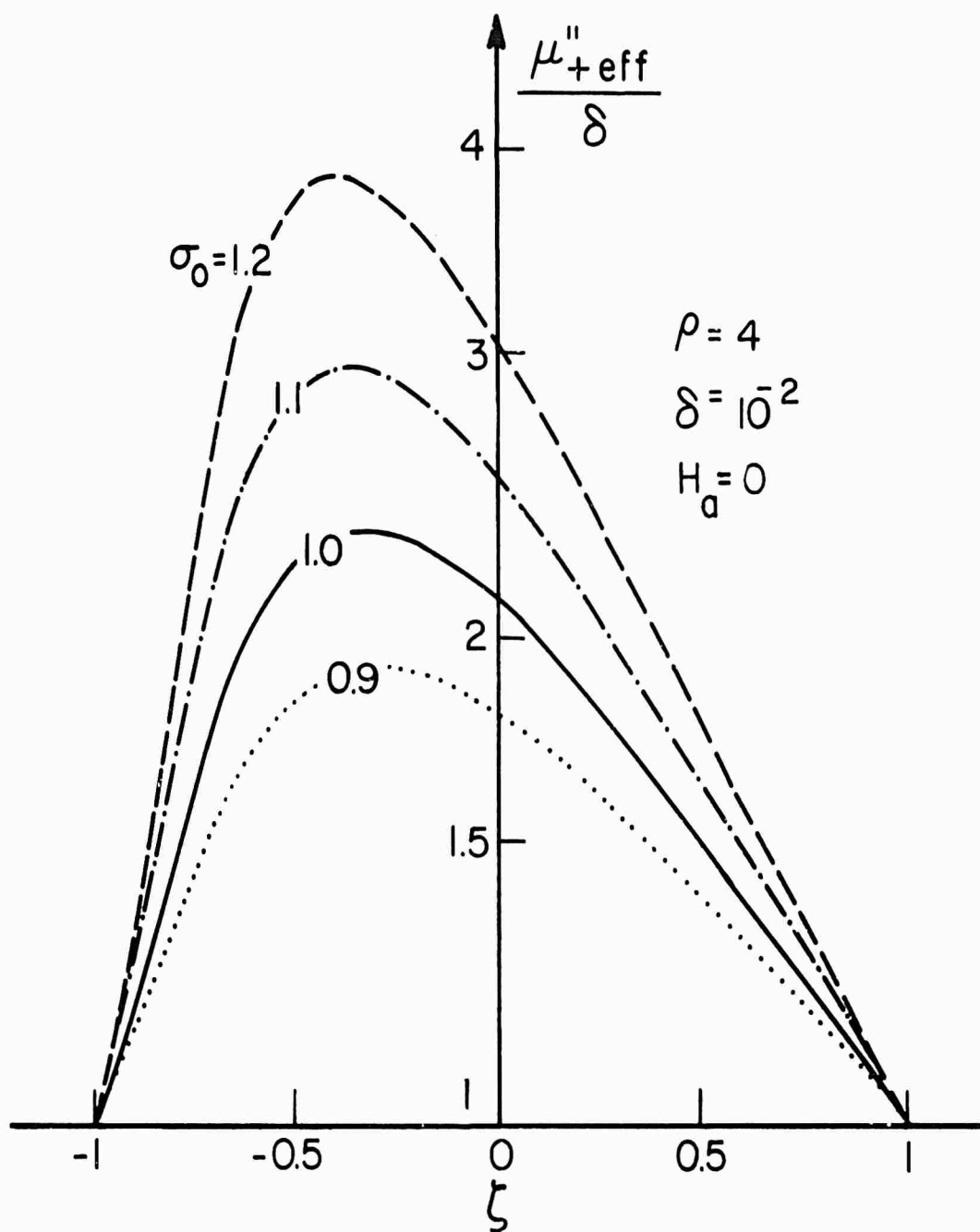


Fig. 8 Absorption coefficient for positive circular polarization μ''_{+eff} vs reduced magnetization ζ . The curves apply to a three-domain configuration for $\rho = 4$, $\delta = 10^{-2}$, and $\omega_M/\omega = 0.9 - 1.2$, and $H_a = 0$.

can readily be evaluated by hand. For $N = 6, 10, 20, 40, 80$ they were evaluated numerically on a computer. For simplicity σ was taken as real. Thus the resultant μ_{eff} and κ_{eff} are also real. The results of the calculation for $\sigma = 0.9$ are shown in Figs. 9 and 10. The case $N = 2$ is, of course, identical with the three-domain case for $\rho = 0$. Figure 9 shows the dependence of μ'_{eff} upon ζ . With increasing N the curve becomes more nearly symmetric in ζ . As expected from the general discussion in Section 3a the minimum value of μ_{eff} is independent of N .

The variation of κ'_{eff} with ζ is shown in Fig. 10. Also shown in this graph is the prediction of Rado's theory. It appears that κ'_{eff} as calculated on the basis of the present theory approaches Rado's value in the limit of large N .

The remarks concerning hysteresis of the variation of μ_{eff} and κ_{eff} with ζ made in connection with the three-domain case apply equally well in the present case. The curves shown are based upon the assumption that the core domain is magnetized down.

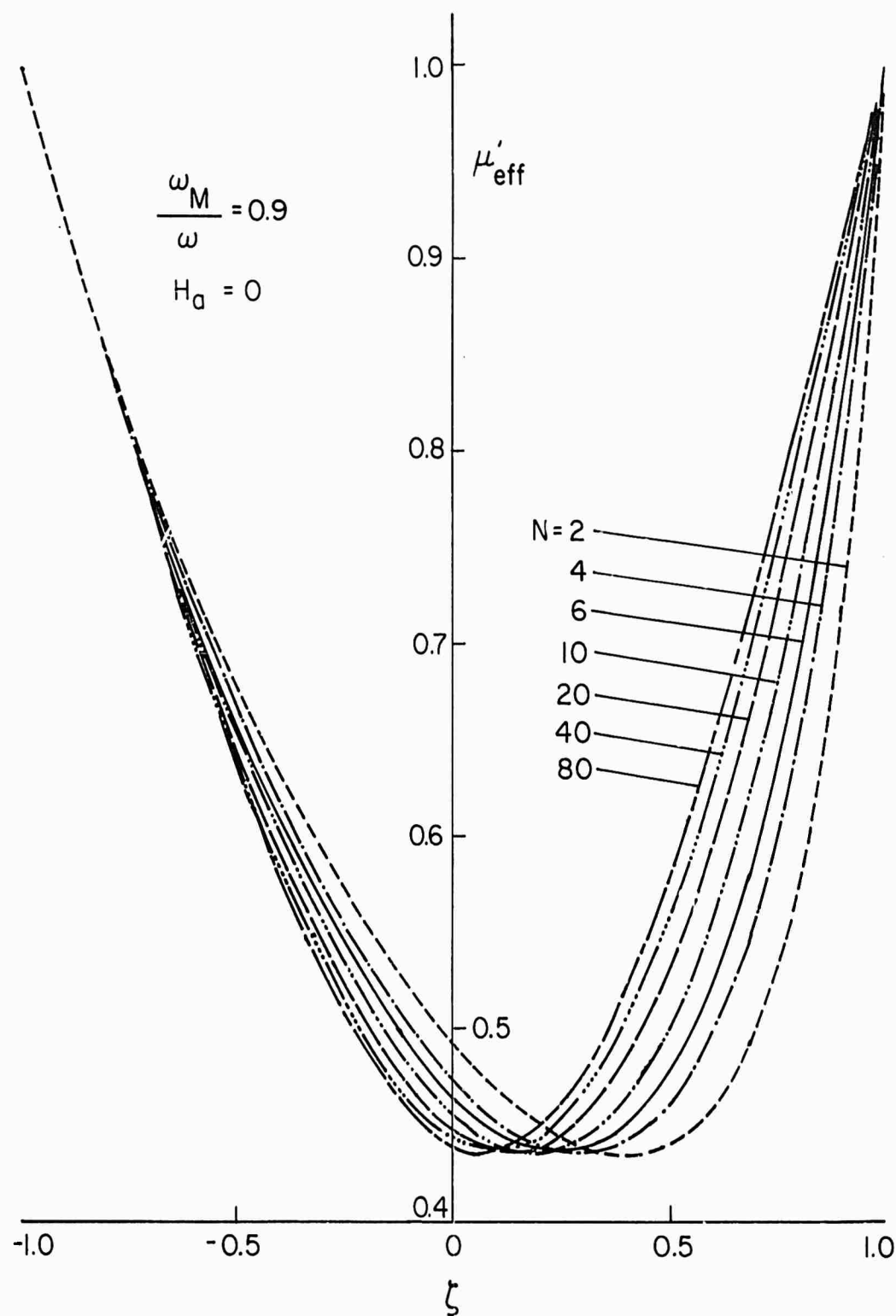


Fig. 9 Real part of the diagonal component of the effective permeability μ'_{eff} vs reduced magnetization ζ . The curves apply to configurations comprising an even number (N) of domains, with domains of the same type having equal volume, $\omega_M/\omega = 0.9$, $H_a = 0$.

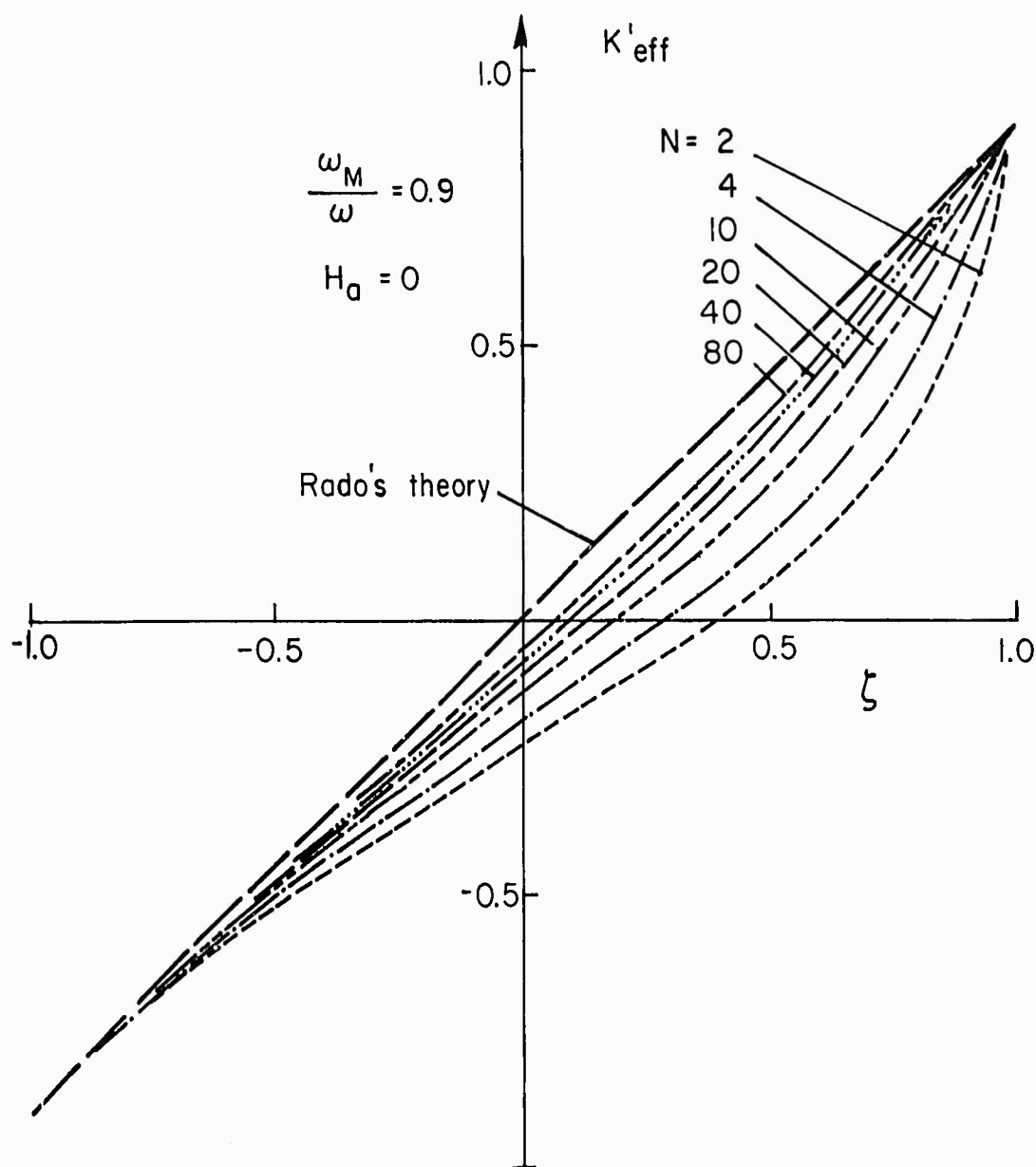


Fig. 10. Real part of the off-diagonal component of the effective permeability μ'_{eff} vs reduced magnetization ζ . The curves apply to configurations comprising an even number (N) of domains, with domains of the same type having equal volume, $\omega_M/\omega = 0.9$, $H_a = 0$.

4. DISCUSSION

The theory described in the present paper differs from those previously proposed primarily in that attention is first focussed on the determination of the local rf magnetic field. This field is calculated substantially rigorously, subject only to the quasi-static approximation. In order to carry out the calculation it was necessary to assume a simple domain configuration. In particular the explicit calculations of the effective permeability described in Sec. 3b and c are based upon the assumption of very idealized configurations. Thus the results of the calculation should be interpreted with appropriate caution.

In actuality the sample will contain very many domains of different size, and they may be oriented in many different ways. For such a domain configuration the resonant frequencies of the proper modes of vibration are very likely distributed over a fairly wide frequency band. Thus the absorption coefficients, considered as functions of magnetization (ζ), will very likely not show sharp peaks as deduced on the basis of the three-domain (see Figs. 7 and 8). The hysteresis in the μ_{eff} vs ζ and κ_{eff} vs ζ curves may be expected to be considerably smaller in a realistic domain configuration than in the three-domain configuration assumed in Sec. 3b. This is confirmed by the results obtained for the many domain model discussed in Sec. 3c (compare Figs. 9 and 10).

For a comparison with experimental data some allowance must be made for the fact that the domains may be oriented along directions other than the z-axis as assumed throughout the present paper. The general method developed in the present paper can also be applied to such domain configurations, but the detailed calculation becomes considerably more involved.

For the completely demagnetized state the random orientation of the domains can easily be taken into account in an approximate fashion. In

this case the off-diagonal components of the permeability tensor vanish. If only up- and down-domains are present the diagonal components corresponding to the x- and y-directions are given by Eq. (30) and that corresponding to the z-direction equals unity. The average permeability for random orientation may then be expected to be given approximately by the average of the permeabilities applicable in the three principal directions. This yields, according to Eq. (30), as the average (isotropic) permeability in the demagnetized state

$$\mu_{\text{demag}} = \frac{2}{3} \left[\frac{(\omega/\gamma)^2 - (H_a + 4\pi M_0)^2}{(\omega/\gamma)^2 - H_a^2} \right]^{\frac{1}{2}} + \frac{1}{3} \quad (44)$$

For $\gamma(H_a + 4\pi M_0)/\omega \ll 1$ in particular

$$\mu_{\text{demag}} = 1 - \frac{1}{3} \frac{\omega_M (\omega_M + 2H_a)}{\omega^2} \quad (45)$$

This result resembles the interpolation formula proposed by Bady,⁶ which has been found to agree quite well with the observations.

The permeability defined by Eq. (44) is real for $\omega > \gamma(4\pi M_0 + H_a)$ and imaginary for $\gamma H_a < \omega < \gamma(4\pi M_0 + H_a)$. It thus accurately describes the onset of low-field loss. With suitable correction to allow for a finite line-width and possible variations of the anisotropy field from one domain to the other, Eq. (44) has been found to agree quite well with the observed behavior of μ' and μ'' in the demagnetized state for frequency between approximately 0.3 GHz and 10 GHz. For lower frequencies the susceptibility arising from domain-wall displacement, which is not taken into account in the present theory, apparently becomes important.

The theory described in the present paper accounts qualitatively for many of the phenomena observed in partially magnetized ferrites at microwave frequencies. These phenomena include:

1. The onset of low field loss near $\omega_M/\omega = 1$,
2. The variation of κ'_{eff} and μ'_{eff} with net magnetization, in particular the hysteresis observed in this dependence,
3. The variation of μ'_{eff} and μ''_{eff} in the demagnetized state with ω_M/ω (see Eq. 44),
4. The variation of $\mu''_{+\text{eff}}$ and $\mu''_{-\text{eff}}$ with net magnetization, in particular the fact that the absorption peak occurs on the anti-Larmor side.
5. The fact that for $\omega_M/\omega \lesssim 0.5$ the two absorption coefficients for circular polarization become nearly equal, i. e. ,

$$\kappa''_{\text{eff}} \ll \mu''_{\text{eff}}.$$

A detailed comparison of experimental data with the theory will be presented as a separate publication.

APPENDIX II-A, Derivation of Eq. (29)

Let the cross-sectional area of the n^{th} domain be

$$a_n = \pi(r_n^2 - r_{n-1}^2) \quad (\text{A1})$$

and assume that the total number of domains (N) is even. Then according to Eqs. (24) and (28)

$$\frac{\mu_{\text{eff}}}{\mu} = 1 + \sigma \frac{a_1 A_1 + a_3 A_3 + \cdots + a_{N-1} A_{N-1} - [a_2 A_2 + a_4 A_4 + \cdots + a_N A_N]}{a_1 A_1 + a_3 A_3 + \cdots + a_{N-1} A_{N-1} + [a_2 A_2 + a_4 A_4 + \cdots + a_N A_N]} \quad (\text{A2})$$

Using Eq. (26) this result may alternatively be written as

$$\frac{\mu_{\text{eff}}}{\mu} = 1 + \sigma \frac{S_{11}(\sigma) - T_{11}(\sigma)}{S_{11}(\sigma) + T_{11}(\sigma)} \quad (\text{A3})$$

where $S_{11}(\sigma)$ and $T_{11}(\sigma)$ are the (1, 1) components (i. e., first row, first column) of the matrices

$$\begin{aligned} \underline{S}(\sigma) &= a_1 \underline{1} + a_3 \underline{M}_2 \underline{M}_1 + \cdots + a_{N-1} \underline{M}_{N-2} \cdots \underline{M}_1 \\ \underline{T}(\sigma) &= [a_2 \underline{1} + a_4 \underline{M}_3 \underline{M}_2 + \cdots + a_N \underline{M}_{N-1} \cdots \underline{M}_2] \underline{M}_1 \end{aligned} \quad (\text{A4})$$

Using the definition (27) of the matrices \underline{M}_n it can readily be shown that

$$\begin{aligned} S_{11}(\sigma) &= F(\sigma) \\ T_{11}(\sigma) &= (1 + \sigma) G(\sigma) \end{aligned} \quad (\text{A5})$$

where $F(\sigma)$ and $G(\sigma)$ are both even functions of σ . Thus according to Eq. (A3)

$$\frac{\mu_{+ \text{ eff}}}{\mu} = (1 + \sigma) \frac{F(\sigma) + (1 - \sigma) G(\sigma)}{F(\sigma) + (1 + \sigma) G(\sigma)} \quad (\text{A6})$$

$\mu_{- \text{ eff}}$ is now obtained by replacing σ with $-\sigma$. Hence

$$\frac{\mu_{+ \text{ eff}} \mu_{- \text{ eff}}}{\mu^2} = 1 - \sigma^2 \quad (\text{A7})$$

which is equivalent with Eq. (29).

If N is odd slight differences in the notation are required, but substantially the same proof still holds.

APPENDIX II-B, Derivation of Eq. (42)

With

$$\begin{aligned} a_1 = a_3 = \dots = a_{N-1} &= q \pi r_2^2 \\ a_2 = a_4 = \dots = a_N &= p \pi r_2^2 \end{aligned} \quad (A8)$$

Equation (A4) can be written as

$$\begin{aligned} \tilde{S}(\sigma) &= q \pi r_2^2 [1 + \tilde{P}_2 + \tilde{P}_4 \tilde{P}_2 + \dots + \tilde{P}_{N-2} \dots \tilde{P}_2] \\ \tilde{T}(\sigma) &= p \pi r_2^2 [1 + \tilde{P}_3 + \tilde{P}_5 \tilde{P}_3 + \dots + \tilde{P}_{N-1} \dots \tilde{P}_3] \tilde{M}_1 \end{aligned} \quad (A9)$$

where

$$\tilde{P}_n = \tilde{M}_n \tilde{M}_{n-1} \quad (A10)$$

Using the definition (26) of \tilde{M}_n one obtains for integer n

$$\begin{aligned} \tilde{P}_{2n} &= \begin{pmatrix} 1 - \sigma^2 \frac{p}{n} & (1 - \sigma) \sigma \frac{p}{r_2^2 n (n - p)} \\ (1 + \sigma) \sigma r_2^2 p & 1 + \sigma^2 \frac{p}{n - p} \end{pmatrix} \\ \tilde{P}_{2n+1} &= \begin{pmatrix} 1 - \sigma^2 \frac{q}{n + q} & - (1 + \sigma) \sigma \frac{q}{r_2^2 n (n + q)} \\ - (1 - \sigma) \sigma r_2^2 q & 1 + \sigma^2 \frac{q}{n} \end{pmatrix} \end{aligned} \quad (A11)$$

$$M_1 = \begin{bmatrix} 1 + \sigma & \sigma q^{-1} r_2^{-2} \\ -\sigma q r_2^2 & 1 - \sigma \end{bmatrix} \quad (A12)$$

If we define $f_N(\sigma)$ and $g_N(\sigma)$ (symmetric functions of σ) by

$$\begin{aligned} S_{11}(\sigma) &= q \pi r_2^2 f_N(\sigma) \\ T_{11}(\sigma) &= p \pi r_2^2 (1 + \sigma) g_N(\sigma) \end{aligned} \quad (A13)$$

the effective circular permeability is according to Eq. (A3)

$$\begin{aligned} \frac{\mu_{+eff}}{\mu} &= 1 + \sigma \frac{q f_N(\sigma) - p(1 + \sigma) g_N(\sigma)}{q f_N(\sigma) + p(1 + \sigma) g_N(\sigma)} \\ &= 1 + \sigma \frac{y(\sigma) - 1 - \sigma}{y(\sigma) + 1 + \sigma} \end{aligned} \quad (A14)$$

where $y(\sigma)$ is defined by Eq. (43). Equation (42) is now obtained by using Eqs. (11) and (12).

REFERENCES

1. R. C. LeCraw and E. G. Spencer, IRE Convention Record Part V, 66 (1956).
2. R. C. LeCraw and E. G. Spencer, J. Appl. Phys. 28, 399 (1957).
3. F. Sandy and J. J. Green, J. Appl. Phys. 38, 1413 (1967).
4. L. Courtois and A. Deschamps, Compl. rend. 264, 573 (1967); 264, 1333 (1967).
5. J. J. Green, C. E. Patton, and F. Sandy, "Microwave Properties of Partially Magnetized Ferrites," Final Report RADC-TR-68-312, August 1968.
6. I. Bady, J. Appl. Phys. (to be published).
7. G. T. Rado, Phys. Rev. 89, 529 (1953).
8. G. T. Rado, IRE Trans. AP-4, 512 (1956).
9. R. F. Soohoo, IRE Convention Record V, 84 (1956).
10. J. L. Allen, Ph.D. Thesis, Georgia Inst. Tech. (1966).
11. F. Sandy, Raytheon Techn. Memo T-815, March 1969.
12. D. Polder and J. Smit, Rev. Mod. Phys. 25, 89 (1953).
13. T. A. Kriz and T. K. Ishii, J. Appl. Phys. 39, 5029 (1968).
14. See, for instance, C. E. Patton, Phys. Rev. (to be published).
15. R. L. Walker, Phys. Rev. 105, 390 (1957).
16. E. Schlömann and R. I. Joseph, Raytheon Technical Report R-68 (March 1968), to be published as part of Magnetic Properties of Materials, J. Smit, ed., McGraw-Hill Inter-University Series.

Unclassified

Security Classification

DOCUMENT CONTROL DATA - R & D		
(Security classification of title, body of abstract and indexing annotation must be entered when the overall report is classified)		
1. ORIGINATING ACTIVITY (Corporate author)		2a. REPORT SECURITY CLASSIFICATION
Raytheon Company, Research Division 28 Seyon St Waltham, Mass 02154		NA (Unclassified)
3. REPORT TITLE		2b. GROUP
Characterization of the Microwave Tensor Permeability of Partially Magnetized Materials		NA
4. DESCRIPTIVE NOTES (Type of report and inclusive dates)		
Semiannual Technical Report, 5 August 1968 - 5 February 1969		
5. AUTHOR(S) (First name, middle initial, last name)		
Jerome J. Green, Ernst Schlömann, Frank Sandy, Joseph Saunders		
6. REPORT DATE	7a. TOTAL NO. OF PAGES	7b. NO. OF REFS
February 1969	71	5
8a. CONTRACT OR GRANT NO.	8a. ORIGINATOR'S REPORT NUMBER(S)	
F30602-69-C-0026	S-1143	
b. PROJECT NO.	9b. OTHER REPORT NO(S) (Any other numbers that may be assigned this report)	
A0550	RADC-TR-69-93	
c.		
d.		
10. DISTRIBUTION STATEMENT		
This document is subject to special export controls and each transmittal to foreign governments, foreign nationals or representatives thereto may be made only with prior approval of RADC (EMATE) Griffiss AFB NY		
11. SUPPLEMENTARY NOTES		12. SPONSORING MILITARY ACTIVITY
Monitored by Rome Air Development Center (EMATE) Griffiss Air Force Base, N. Y. 13440		Advanced Research Projects Agency Washington, D. C. 20301
13. ABSTRACT		
<p>The loss for a partially magnetized material can be characterized by μ'' of the completely demagnetized state if $\omega_M/\omega \leq 0.7$. Results are presented for a number of YIG with Al and Gd substitutions and MgMn spinels with Al substitutions. μ'' has been measured at frequencies of 5.5, 7.3, 9.0, 11.4, 13.8, 16.9 GHz. The results can be approximated by a relation $\mu'' = A(\omega_M/\omega)^N$. The YAlIG are low loss, MgMn AlF slightly higher, and the YGdAlIG considerably higher in loss. Two theoretical models have been developed which are an improvement over Rado's theory and give qualitative description of the partially magnetized permeability tensor.</p> <p>High power parallel pump measurements have been made on the same materials at frequencies of 5.5 and 9.2 GHz and at fields of 0, $4\pi M_s/3$ and H_{min}. These materials have the same ranking with respect to threshold as they have for low power loss.</p>		

DD FORM 1473

NOV 63

REPLACES DD FORM 1473, 1 JAN 64, WHICH IS OBSOLETE FOR ARMY USE.

Unclassified

Security Classification

Unclassified

Security Classification

14. KEY WORDS	LINK A		LINK B		LINK C	
	ROLE	WT	ROLE	WT	ROLE	WT
Partially magnetized Permeability tensor Phase shifter materials High power threshold Insertion loss properties						

Unclassified

Security Classification